Southern Plains Transportation Center
CYCLE 1

FINAL REPORT

2023–2024

USDOT BIL Regional UTC
Region 6

Use of Distributed Acoustic Sensing for Structural Health Monitoring of Asphalt Pavements

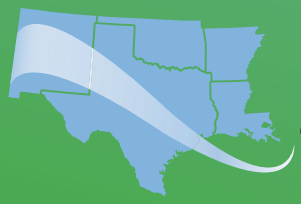

SOUTHERN PLAINS
TRANSPORTATION CENTER

Disclaimer

The contents of this report reflect the views of the authors, who are responsible for the facts and accuracy of the information presented herein. This document is disseminated under the sponsorship of the Department of Transportation University Transportation Centers Program, in the interest of information exchange. The U.S. Government assumes no liability for the contents or use thereof.

Technical Report Documentation Page

1. Report No. CY1-UTEP-01	**2. Government Accession No.**	**3. Recipient's Catalog No.**
4. Title and Subtitle Use of Distributed Acoustic Sensing for Structural Health Monitoring of Asphalt Pavements		**5. Report Date** September 2024
		6. Performing Organization Code
7. Author(s) Sebastian Morales, 0009-0009-8185-8482, https://orcid.org/0009-0009-8185-8482 Cesar Tirado, 0000-0002-8784-3347, https://orcid.org/0000-0002-8784-3347 Soheil Nazarian, 0000-0002-2622-1261, https://orcid.org/0000-0002-2622-1261		**8. Performing Organization Report No.**
9. Performing Organization Name and Address Center for Transportation Infrastructure Systems, 500 W. University Ave., Metallurgy Building M-104 The University of Texas at El Paso El Paso, TX, 79968		**10. Work Unit No. (TRAIS)**
		11. Contract or Grant No. 69A3552348306
12. Sponsoring Agency Name and Address Southern Plains Transportation Center 202 West Boyd St., Room 213B The University of Oklahoma Norman, OK 73019		**13. Type of Report and Period Covered** Final Report 11/01/2023- 1/15/2025
		14. Sponsoring Agency Code

15. Supplementary Notes
Conducted in cooperation with the U.S. Department of Transportation as a part of University Transportation Center (UTC) program.

16. Abstract
This research investigates the feasibility of utilizing Distributed Fiber Optic Sensing (DFOS) technology to monitor strain within pavement structures. Unlike traditional sensors, DFOS provides high-resolution strain measurements along the entire length of an optical fiber, enabling continuous monitoring of pavement behavior under traffic loading. The study involved calibrating a DFOS system using a dedicated jig and implementing it within a laboratory-scale accelerated pavement testing setup. Challenges related to sensor installation, compaction, and slab support were encountered and addressed. Results demonstrated the ability of DFOS to capture high-resolution strain distributions within asphalt slabs subjected to simulated traffic loads, surpassing traditional methods and with readings every 2.6 mm along the fiber. The study concludes that DFOS offers significant advantages in real-time pavement monitoring, improving the accuracy and efficiency of data collection for maintenance planning. These findings will support the development of best practices for implementing DFOS systems, equipping pavement engineers with tools for proactive road management and optimizing infrastructure maintenance strategies.

17. Key Words Distributed Fiber Optics Sensing (DFOS), Distributed Strain Sensing (DSS), Pavements, Pavement Responses, Strain.	**18. Distribution Statement** No restrictions. This publication is available at www.sptc.org and from the NTIS.

19. Security Classification (of this report) Unclassified	**20. Security Classification (of this page)** Unclassified	**21. No. of Pages** 53	**22. Price** N/A

Form DOT F 1700.7 (8-72) Reproduction of completed page authorized

USE OF DISTRIBUTED FIBER OPTIC SENSING (DFOS) FOR STRUCTURAL HEALTH MONITORING OF ASPHALT PAVEMENTS

FINAL REPORT
SPTC Project Number: CY1-UTEP-01

Submitted by
Dr. Cesar Tirado (PI)
Dr. Soheil Nazarian (Co-PI)
Sebastian Morales (Graduate Student)
School of Civil Engineering and Environmental Science (CEES)
The University of Texas at El Paso

Prepared for
Southern Plains Transportation Center
The University of Oklahoma
Norman, OK

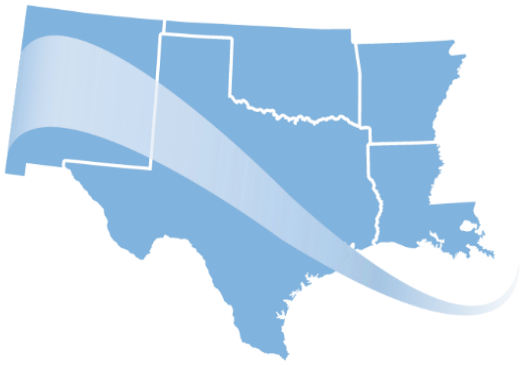

SOUTHERN PLAINS
TRANSPORTATION CENTER

January 2025

Acknowledgments

The authors would like to express their gratitude to Southern Plains Transportation Center for providing financial support for this study. The authors would like to extend their gratitude to the Center for Transportation Infrastructure Systems (CTIS) staff for their invaluable support and dedication in assisting with the laboratory test setup and facilitating the successful completion of the testing.

Table of Contents

List of Tables

List of Figures

List of Equations

List of Abbreviations and Acronyms

DOT	Department of Transportation
FHWA	Federal Highway Administration
NTL	National Transportation Library
ROSA P	Repository & Open Science Access Portal
DFOS	Distributed Fiber Optic Sensing
DTS	Distributed Temperature Sensing
DAS	Distributed Acoustic Sensing
DSS	Distributed Strain Sensing
MMLS	Model Mobile Load Simulator
OFDR	Optical Frequency Domain Reflectometry
LC/APC	Lucent Connector/Angled Physical Contact
SMF	Single Mode Fiber
TLS	Tunable Laser Source
PG	Performance Graded

Executive Summary

This research investigated the feasibility and potential of Distributed Fiber Optic Sensing (DFOS) technology for real-time pavement monitoring. DFOS offers significant advancement over traditional point-based sensors by providing continuous strain measurements along the entire length of an optical fiber, enabling high-resolution data collection and improved spatial coverage. By embedding DFOS technology into pavement structures, this research aims to provide a preliminary evaluation of the use of this technology that potentially eventually can be utilized for road asset management for transportation agencies, particularly within Region 6, by enabling more accurate and timely assessments of pavement conditions.

The study demonstrated the successful implementation of distributed strain sensors (DSS), a type of DFOS, for measuring strain responses in asphalt slabs under simulated traffic loads. The research involved developing a tool for the calibration of strain sensors, calibrating the strain sensing system, and exploring methods for embedding fiber optic cables into pavement materials. Results showed that the fiber optic sensors capture strains at high spatial resolution (every 2.6 mm), providing detailed insights into pavement behavior.

While the study demonstrated the potential of fiber optic sensors, it was also found that strain measurements are highly susceptible to the sensor bonding technique and problems from the experimental setup. Moreover, other challenges were identified, such as data management and data reduction. Future research should focus on addressing these limitations, including the development of robust data reduction algorithms, optimization of sensor embedding techniques, assessment of measurement variability, and sensitivity to pavement distress. Moreover, the limitations in the sampling rate complicate the measurement of responses of rapid response tests, such as lightweight deflectometer testing.

The successful implementation of DFOS technology for pavement monitoring has the potential to revolutionize road asset management practices. By enabling real-time, high-resolution data collection, DFOS can improve the accuracy of pavement condition assessments, optimize maintenance strategies, and ultimately lead to more cost-effective and efficient road infrastructure management.

Chapter 1. Introduction

1.1 Problem Statement

The main objective of this research is to gain an understanding and develop tools to use distributed fiber optics sensing (DFOS) for monitoring the performance of pavement layers under traffic conditions. DFOS is an advanced non-invasive, real-time sensing technology that can overcome many limitations of traditional gauges. As such, this technology steps beyond the traditional methods for the characterization of in situ materials that make use of embedded sensors such as strain gauges, geophones, or accelerometers to obtain point measurements at specific locations by allowing significantly improved spatial coverage and refined resolution for capturing pavement materials responses under traffic loadings without the need for traffic control. Moreover, fiber optic sensors are insensitive to electromagnetic noise, resistant to corrosion and high-pressure and high-temperature conditions, and do not require electronics along the optical path. These sensors can measure physical properties such as temperature (via Distributed Temperature Sensing or DTS), vibration (via Distributed Acoustic Sensing or DAS), and strain (via Distributed Strain Sensing or DSS), simultaneously along the entire fiber. The results from this study will lead to the development of best practices to implement this innovative technology that will give pavement engineers insight into the pavement condition. It is expected that DOTs in Region 6 can potentially use the outcomes of this technology for more effective asset management.

1.2 Objectives and Scope of Work

The primary objective of this research was to explore the potential of Distributed Fiber Optic Sensing (DFOS) systems for continuous, real-time monitoring of pavement strain under traffic loading conditions. This study aimed to establish a robust methodology for embedding DFOS systems into pavement structures. By capturing strain data with high spatial resolution, this research sought to improve pavement condition assessment and optimize maintenance strategies.

The scope of work included the selection of appropriate fiber optic strain cables that could withstand high loads and strains without failure, as well as the development of installation procedures to ensure seamless integration with asphalt pavements. The proper calibration of the DFOS system was a critical component of this study, involving the fabrication of an aluminum jig subjected to controlled loading conditions to derive accurate strain coefficients. The research also involved embedding DFOS cables into asphalt slabs compacted using a Model Mobile Load Simulator (MMLS) to replicate traffic-induced stress.

The research encompasses multiple stages, including:

1. **Cable Selection and Preparation:** Identifying steel-reinforced fiber optic strain cables suitable for harsh pavement conditions and ensuring compatibility with the ODiSI6 sensor interrogator system.
2. **Calibration Procedures:** Conducting a three-point bending test on an aluminum jig to establish a correlation between spectral shift data and known strain values. Calibration ensures accurate strain measurements during traffic simulations.
3. **Installation in Asphalt Slabs:** Developing precise methods to create grooves in asphalt slabs to house the DFOS cables. The cables are secured using epoxy glue to prevent movement during loading tests.

4. **Traffic Simulation and Data Collection:** Utilizing the MMLS to apply dynamic loads on instrumented asphalt slabs. Real-time strain data is captured and analyzed using the ODiSI6 system, with strain readings recorded at high acquisition rates and short gauge pitches for detailed spatial resolution.
5. **Data Reduction and Analysis:** Applying data reduction techniques to manage the large datasets generated by DFOS systems. Methods such as moving average filters are explored to enhance data usability without sacrificing accuracy.

This comprehensive approach ensured that the DFOS system was thoroughly tested and validated for practical applications in pavement monitoring. The outcomes of this research are expected to provide transportation agencies with new tools for proactive maintenance, reducing costs, and extending the lifespan of road infrastructure.

1.3 Organization of Report

This report is structured into nine chapters to address the findings of the research conducted on utilizing DOFS technology for real-time pavement strain monitoring. The report is structured into nine chapters, followed by the reference list and an appendix containing supporting information. The chapters are listed below:

- **Chapter 1: Introduction.** This chapter establishes the rationale for the research by defining the problem statement, outlining the project objectives, and providing the organization of the report.
- **Chapter 2: Literature Review.** This chapter presents a brief review of existing literature relevant to the research. It explores relevant studies on pavement monitoring techniques, focusing on this emerging technology of DFOS. The review also discussed the application of DFOS in other fields.
- **Chapter 3: Methodology for Testing with Fiber Optic Strain Sensors.** This chapter provides a detailed description of the research methodology, describing the instrumentation setup. It covers the selection of materials, and components, the design and construction of test specimens, and the instrumentation and data acquisition procedures.
- **Chapter 4: Calibration of Fiber Optic Strain Sensors.** This chapter focuses on the calibration process for the strain sensors. It details the development and implementation of a dedicated calibration jig and compares the results with theoretical predictions to define the calibration procedure.
- **Chapter 5: Accelerated Pavement Testing and Results using DFOS and MMLS.** This chapter discusses the test setup using MMLS and presents the results of the accelerated pavement testing conducted using the MMLS and the embedded DFOS sensors. It analyzes the strain data collected and discusses the observed trends, variations, and complications.
- **Chapter 6: Conclusions and Recommendations.** This chapter summarizes the key findings and conclusions of the research. It discusses the strengths and limitations of the DFOS technology for pavement strain monitoring and provides recommendations for future research directions and improvements to the methodology.
- **Chapter 7: Implementation of Project Outputs.** This chapter provides specific guidelines for calibrating and installing distributed fiber optic strain sensors that can be used for real-time pavement strain monitoring, based on the insights and experiences gained during the research.

- **Chapter 8: Technology Transfer and Community Engagement and Participation (CEP) Activities.** This chapter documents the outreach and engagement activities undertaken by the research team, including STEM activities with the community and high school students.
- **Chapter 9: Invention Disclosures and Patents, Publications, Presentations, Reports.** This chapter provides a list of the presentations generated as a result of the research project.
- **References:** This section provides a comprehensive list of all sources cited within the report, adhering to a consistent citation style.
- **Appendix A: Code to Visualize Strain Measurements.** This appendix includes the Matlab code used for visualizing the strain measurements obtained from the DFOS system.

Chapter 2. Literature Review

2.1 Introduction

Distributed Fiber Optic Sensing (DFOS) is an advanced non-invasive, real-time sensing technology that can overcome many limitations of traditional gauges (Johannesen et al. 2012). As such, this technology steps beyond the traditional methods for the characterization of in situ materials that make use of embedded sensors such as strain gauges, geophones, or accelerometers to obtain point measurements at specific locations by allowing significantly improved spatial coverage and refined resolution for capturing pavement materials responses under traffic loadings without the need for traffic control. Moreover, fiber optic sensors are insensitive to electromagnetic noise, resistant to corrosion and high-pressure and high-temperature conditions, and do not require electronics along the optical path. These sensors can measure physical properties such as temperature (via Distributed Temperature Sensing or DTS), vibration (via Distributed Acoustic Sensing or DAS), and strain (via Distributed Strain Sensing or DSS), simultaneously along the entire fiber (Ekechukwu and Sharma, 2021).

2.2 Distributed Fiber Optic Sensing

Optical scatterings in fiber are generally classified into elastic and inelastic scattering. Rayleigh scattering, an example of elastic scattering, occurs when light interacts with density fluctuations in the silica fiber's molecular structure, causing a scattered signal without frequency shifts (Ghazali et al., 2024). This principle is foundational to Distributed Acoustic Sensing (DAS), a key subset of DFOS technology, which enables real-time monitoring along the entire fiber length without relying on discrete sensors at specific locations. This capability makes DAS invaluable in civil engineering applications where continuous structural monitoring is essential to identify anomalies, deformations, or weaknesses (Ghazali et al., 2024).

The layout and coupling method of fiber optic cables significantly influence the quality of monitoring data in DAS systems. Various cable installation techniques are tailored to different monitoring conditions, highlighting the importance of selecting appropriate layouts for achieving accurate data (Zhu et al., 2022). Proper installation ensures the fiber is well coupled with the structure it monitors, minimizing signal loss and improving data precision.

2.3 Pavement Instrumentation Efforts

The use of fiber optic sensors in pavement engineering has gained increasing attention due to their ability to capture high-resolution strain data over long distances. For asphalt pavements, the most common installation technique involves embedding packaged Fiber Bragg Grating sensors into slotted pavement sections, secured with epoxy adhesive to maintain bond integrity (Wang et al., 2023). This embedding technique has been proven effective in detecting high-precision vehicle vibration signals on highways, further validating its potential for real-world applications (Kou et al., 2024).

However, the survival rate of fiber optic sensors embedded in pavement structures remains a critical challenge. Real traffic conditions introduce variables that can affect sensor durability and data accuracy, necessitating further field tests to refine installation techniques and enhance sensor resilience (Wang et al., 2023). Xiang and Wang (2018) demonstrated that distributed optical fiber sensors effectively measure asphalt pavement strain, with in situ data indicating significant impacts from temperature variations and traffic loads on pavement performance. These

findings underscore the importance of continued improvements in embedding methods to ensure accurate and long-term monitoring.

2.4 Applications of Distributed Fiber Optic Sensing

The applications of DFOS technology in civil engineering are extensive and continue to grow. In pavement monitoring, DFOS systems can detect strain responses to traffic loads and condition changes, providing insights that enhance maintenance planning and road safety. Distributed Acoustic Sensing (DAS) is particularly useful for detecting dynamic interactions, such as vehicle movements and structural vibrations, in real time (Ghazali et al., 2024).

The coupling effect between fiber optic cables and the monitored structures is critical in achieving reliable data collection. Zhu et al. (2022) emphasize that the choice of cable layout directly determines the quality of monitoring data, requiring tailored approaches based on specific infrastructure needs. For road applications, embedding techniques must account for both durability and accuracy, with epoxy adhesives commonly used to secure the sensors in asphalt pavements (Wang et al., 2023).

Moreover, integrating DFOS with other sensing technologies can further improve monitoring accuracy and expand its applications. Recent studies have highlighted the ability of DFOS to provide detailed strain data across entire pavement sections, enabling continuous assessment of road integrity and early detection of potential issues. This capability can optimize road maintenance, reduce repair costs, and improve overall infrastructure management (Xiang & Wang, 2018; Kou et al., 2024). While DFOS technology holds immense promise, ongoing research is necessary to address challenges related to sensor survival rates and data accuracy under real-world conditions.

Chapter 3. Methodology for Testing with Fiber Optic Strain Sensors

3.1 Setup and Instrumentation

This research study utilized a Luna ODiSI 6104 optical distributed sensor interrogator, shown in Figure 1, as the primary system for distributed fiber-optic strain sensing. The ODiSI6 system comprises the following components (shown in Figure 1):

- *Sensor interrogator*: The core unit for acquiring strain measurements.
- *Controller (laptop computer)*: Linux-based system with software to operate the interrogator and analyze collected data.
- *Standoff cable*: Connects the interrogator to the remote modules.
- *Remote modules*: Two modules are included, with one designated for extended-length cables (50 ft or longer).
- *Optical fiber connector cleaner*: Essential for maintaining clean connections.
- *ODiSI power cord*: Provides power to the interrogator.
- *USB3 Type A to B cable*: Connects the sensor interrogator to the controller (laptop).

Figure 1. OdiSI 6104 sensor interrogator components: (1) ODiSI power cord, (2) USB3 type A-to-B cable, (3) sensor interrogator, (4) fiber cleaner, (5) standoff cable, (6) extended length remote module, (7) standard length remote module, and (8) instrument controller (laptop computer).

To support this system, additional equipment was acquired, shown in Figure 2, including:

- NZS-DSS-C02 strain sensing optical cable,
- Patch cables with LC/APC connectors,
- 125 µm coreless termination fiber,
- Swift K33A arc fusion splicer, and
- A fiber optic toolkit comprising a fiber stripper, round cable slitter, Kevlar scissors, tweezers, pliers, and other essential tools for preparing strain gauge sensor connections.

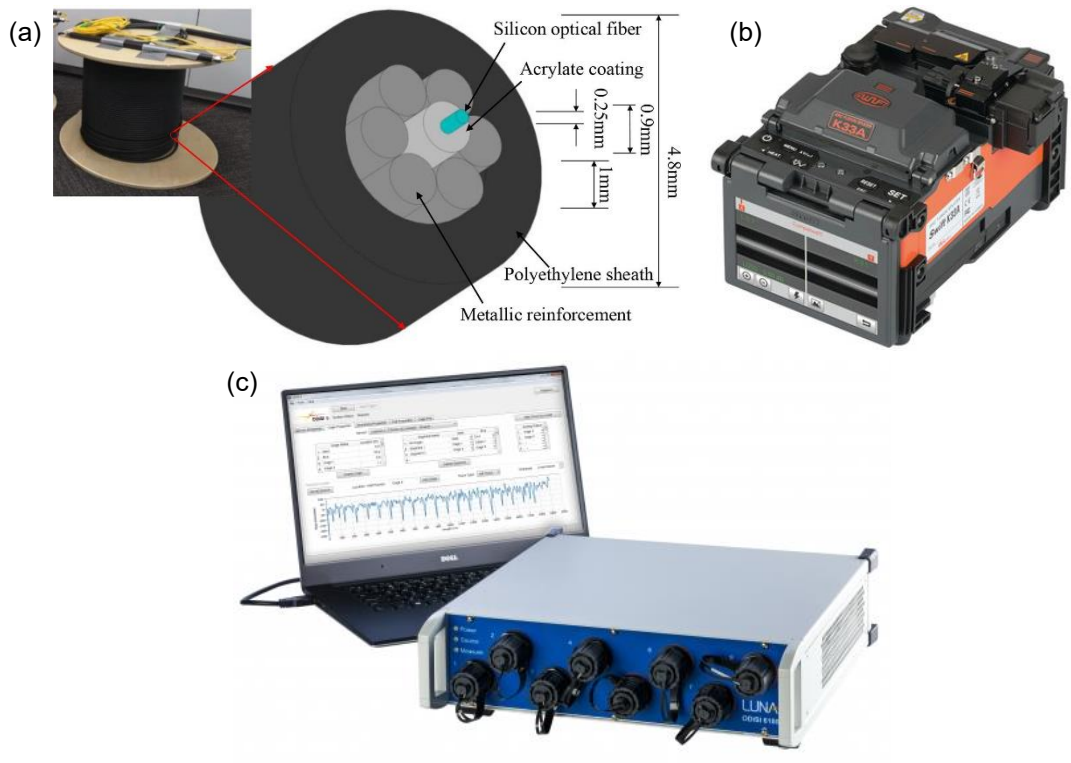

Figure 2. (a) Schematic cross-section of NZS-DSS-C02 strain sensing optical cable (Wang et al. 2023), (b) Swift K33A arc fusion splicer and (c) ODiSI 6104 sensor interrogator.

Various types of strain cables are available for DFOS. A 5 mm diameter NZS-DSS-C02 (non-zero dispersion-shifted fiber) strain sensing optical cable, classified as G.652.B single-mode fiber (SMF), was utilized as the strain sensor to be used in conjunction with the sensor interrogator. This cable, manufactured by NanZee Sensing Technology Ltd., consists of a 1-core G.652.B single-mode fiber with 9/125 µm core/cladding dimensions. Table 1 provides detailed specifications of the sensing cable. Figure 2 illustrates a cross-section of the sensor and its components.

Table 1 – Specifications of NZS-DSS-C02 Strain Sensing Optical Cable

Fiber Type	Single Mode (SMF)	Variant	G.652.B
Diameter (mm)	5.0±0.2	Core/cladding dimensions (με)	9/125
Strain Range	20,000	Operating Temperature (°C)	-20~80
Wavelength Range (nm)	1310 – 1625	Average Loss (dB/km)	0.198
Brillouin Center Frequency (GHz)	10.850	Brillouin Strain Coefficient (MHz/με)	0.0478
Brillouin Temperature Coefficient (MHz/°C)	1.10	Maximum Tensile Breaking Force (N)	≥ 5000
Rayleigh Strain Coefficient (GHz/με)	0.1515	Rayleigh Temperature Coefficient (GHz/°C)	1.5152

This type of sensing cable, featuring a robust design with its steel strand-reinforced, polyethylene (PE)-jacketed protection, has already been utilized in similar studies (Ou 2024; Hubbard et al. 2022), and is able to ensure high survival rates during sensor deployment, making it suitable for instrumentation of pavements. The steel reinforcement helps the cable to be subjected to high loads and strains without causing the cable to fracture. However, to integrate the strain sensing fiber optic cable into the system, end connections must be prepared to accommodate the connector in the module linked to the sensor interrogator channel.

To connect the sensing optical cable to the sensor interrogator, one end of the strain sensor required preparation to accommodate a connector compatible with the interrogator's channels. In this instance, an LC/APC connector was necessary for interfacing with the remote module. Specifications for this connector are provided in Table 2.

Table 2 – Specifications of Sensor Interrogator Connector

Mode	SM	Polishing	APC
Insertion Loss (dB)	≤ 0.3	Ferrule Size (mm)	2.5
Mechanism	Latch Locking	Durability	500 mating cycles

Given that the strain sensor's diameter exceeded the LC/APC connector's boot size, utilizing a pre-terminated patch cable equipped with an LC/APC connector was preferred. To achieve this, a segment of a pigtail was cut, retaining the LC/APC connector at one end. Subsequently, a fusion splicer was employed to join the cut end of the patch cable to the fiber optic sensor. At the other remaining end of the fiber optic sensor, it was necessary to splice a coreless termination fiber to minimize back reflections from unused branches of fiber components.

3.2 Strain Gauge Sensor Preparation

Preparation of the strain gauge sensor is necessary before proceeding with the calibration of the fiber optic sensor. For this purpose, the research team got familiar with the procedure for manually stripping the fiber optic cable, by removing the first 0.900 µm coating and, subsequently, the 0.250 µm acrylate coating covering the fiber optic sensor.

A UCL Swift K33A arc fusion splicer, shown in Figure 3, was then utilized to carefully strip the inner coating and expose the optical fiber core/cladding. The fiber was precisely cleaved at a 90° angle and then fuse-spliced to the patch cable equipped with an LC/APC connector and core termination, which is used to connect to the remote module. The fusion splicer first aligns the core of both fibers. Once aligned, the splicer generates an electric arc that fuses the fibers together. Before fusion, a 60 mm reinforced heat-shrink protective sleeve for single fusion was carefully positioned loosely on one cable. Reinforcement is provided by a 304-grade stainless steel bar that runs along the length of the protective sleeve. Following the fusion of the fiber cores, this sleeve is carefully slid over the splice point, covering completely the exposed cores. The sleeve is then fused in place, securing the splice and providing strength and additional protection to the weak splice point to minimize the risk of damage during handling or deployment.

The next steps consist of splicing the distal end of the fiber optic sensor to a 250 mm long, 125-µm diameter coreless fiber termination, shown in Figure 4. Specifications of the coreless fiber are provided in Table 3. This clear coreless termination fiber acts as a reflector, enabling accurate data collection by reflecting light back from the end of the entire cable for the optical frequency domain reflectometry (OFDR) system. The same process of stripping, cleaving, and splicing was

employed for both the fiber optic strain cable and the coreless fiber termination, utilizing the core alignment fusion splicer.

Figure 3. Fusion splicer showing screen for viewing fusion splicing process.

Figure 4. 125 µm coreless termination fiber.

Table 3 – Specifications of Coreless Termination Fiber

Glass Diameter (µm)	125 +1/-2	Coating Material	Acrylate
Coating Diameter (µm)	250 ± 12.5	Glass Refractive Index	1.467 @ 436 nm
Operating Temperature (°C)	-40 – 85	Return Loss	>65 dB with 0.25 m end cap

3.3 Data Acquisition and Verification of Integrity of Prepared Fiber Optic Strain Sensor

Before calibration and testing, the integrity of the prepared fiber optic strain sensor must be ascertained. This involved accurately identifying the measurable length and detecting any interruptions in measurements caused by fiber damage resulting from sharp bends or indentations. If the sensor is damaged, splicing will be needed to effectively repair disruptions in measurements. To verify the integrity of the sensor, the prepared strain gauge fiber optic sensor

is connected to the interrogator. OFDR capabilities of the ODiSI 6104 system were needed to identify measurable lengths. This system allows to have spatial resolution of 1.3 mm (Ou 2022). The OFDR is based on swept-wavelength coherent interferometry, relying on a tunable laser source (TLS) to interrogate fiber optic sensors. Physical changes in the optical fiber during an external interruption create measurable changes in the light scattering (Sollerv et al. 2006). Once the integrity of the sensor is verified, the strain sensor is calibrated to ensure the system provides accurate measurements.

To enable data acquisition, for calibration and further data acquisition during testing, the following steps were followed:

1. *System and fiber optic sensor activation:* After connecting the fiber optic cable to the ODiSI system, the software automatically recognizes the fiber optic sensor and assigns a unique key to it. Once the strain sensor is recognized by the software, it should be activated to read measurements.
2. *Strain zeroing:* A “strain zeroing” procedure is needed to establish a baseline measurement across the entire sensor length. This is done to zero any strain measurements before loading the asphalt slab with trafficking loads.
3. *System arming and data collection:* The system is then armed, i.e. prepares the system interrogator for running a test, and data collection is initiated. The software will display a real-time graphical representation of strain measurements along the cable length during data acquisition.
4. *Data Navigation and Analysis:*
    - The "touch to locate" function is utilized to determine the distance to a specific point of interest along the cable.
    - Setting a tar can also be used to identify a desired location of the cable and to set it as the initial point for measuring.
    - Target strain thresholds can be enabled to trigger alerts.
5. *Data Pause and Disarming:* Pause and disarm the system when data collection is complete.

Chapter 4. Calibration of Fiber Optic Strain Sensors

This section documents the approach developed for calibrating the DFOS system and acquiring strain measurements using ODiSI6 software and interrogator. Initial calibration efforts involved exploring simpler setups, such as loading simply-supported small thin steel plates with hanging masses with the fiber optic sensor glued with epoxy running longitudinally along the beam. However, these initial approaches were refined, culminating in the development of a dedicated calibration jig for improved accuracy and repeatability.

The dimensions of the aluminum specimen were carefully selected to induce strain levels representative of those anticipated in typical pavement structures when loaded under the experimental setup. A range of layer thicknesses and material properties commonly documented in pavement analysis and design guidelines and software were analyzed using the BISAR software to predict the tensile strain values at the bottom of the asphalt/concrete layers in response to loading scenarios representative of Falling Weight Deflectometer (FWD) tests and 18-kip single-axle truck loads. The results of these simulations confirmed the selection of aluminum specimen thickness to achieve a range of values that reflect the strain levels seen by pavements.

To calibrate the fiber optic strain sensor, the designed calibration jig, seen in Figure 5a, was instrumented with both a conventional strain gauge and the fiber optic strain sensor and was subjected to a three-point bending test. The calibration jig consists of an aluminum plate, fabricated from an 18-in. long, 2-in. thick, and 4-in. wide T-6061 plate, supported by two steel cylinders spaced 12-in. apart, simulating a simply supported beam configuration. A longitudinal groove was machined into the center of the aluminum plate to accommodate the fiber optic sensor and ensure it remained flush with the plate surface. The groove was precisely machined to a diameter of 5 mm to provide a snug fit for the sensor. This assembly was then mounted within an MTS testing system for controlled, monotonic loading in the three-point bending test mode, as shown in Figure 5b. Dynamic loading was applied to the jig, reaching a maximum load of 4000 pounds, inducing both compressive (on top) and tensile strains (at the bottom), as shown in Figure 5b.

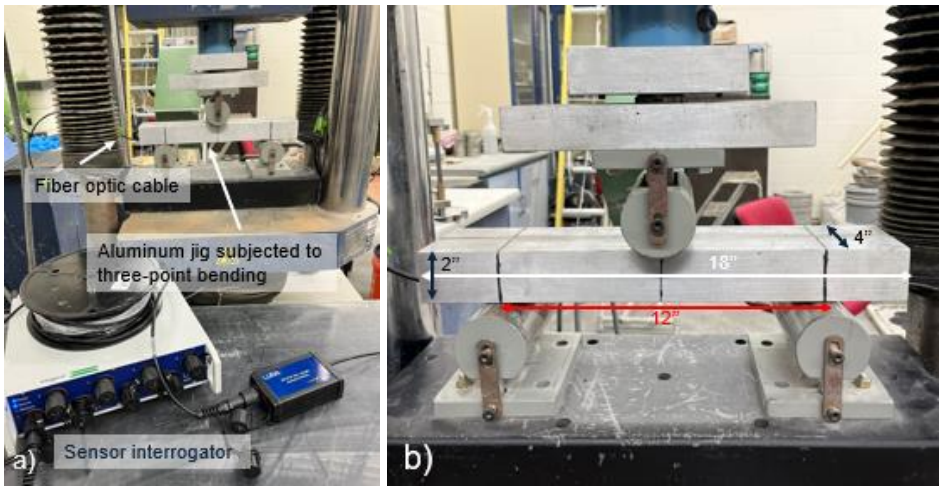

Figure 5. Aluminum jig instrumented with distributed fiber optic sensor connected to the interrogator.

The fiber optic cable was configured to acquire spectral shift data for calibration purposes. This was achieved by connecting the cable to the ODiSI system and creating a unique key within the software's tools options, as described in the previous section. The strain coefficients were initially set to default values and were subsequently adjusted following calibration. Before data collection, the measurement type was changed to "spectral shift" within the "General" options of the software.

Spectral shift, a phenomenon resulting from changes in light scattering within the inner fiber of the optical cable, was observed as the applied load varied. Calibration was performed by plotting the measured spectral shift at each load against the theoretically calculated strain at the corresponding load. Figure 6 shows this calibration curve. The slope of this curve, determined using the linear regression formula, yielded the strain coefficients that were subsequently input into the ODiSI software to calibrate the fiber optic strain cable.

A custom key was created within the sensor interrogator system using the instrument controller software to store the calibrated strain coefficients, as shown in Figure 7. Following calibration, the aluminum jig was dynamically loaded, and the calibrated fiber optic strain sensor recorded strain measurements. A comparison between the calibrated strain measurements obtained from the fiber optic sensor and the theoretically calculated strain values is presented in Figure 8.

The software recognizes the fiber optic strain sensor and will upload the calibration parameters stored in the key when the strain sensor is plugged into the system at a later time to conduct testing. At the present moment, the research team has not identified the need to recalibrate the strain due to the degradation of the sensor connections or splices. However, we have identified the need to calibrate the sensor if damaged, e.g., internal broken core fibers, damaged connections and/or broken fused splices, or damaged coreless fiber, as this is usually exposed and not protected.

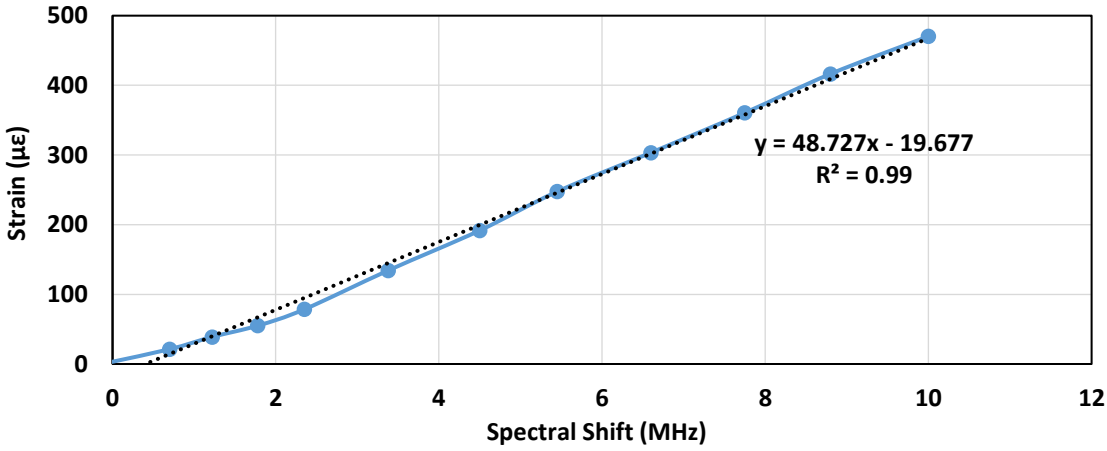

Figure 6. Spectral shift measurements and strain measurements of three-point bending test of aluminum jig specimen.

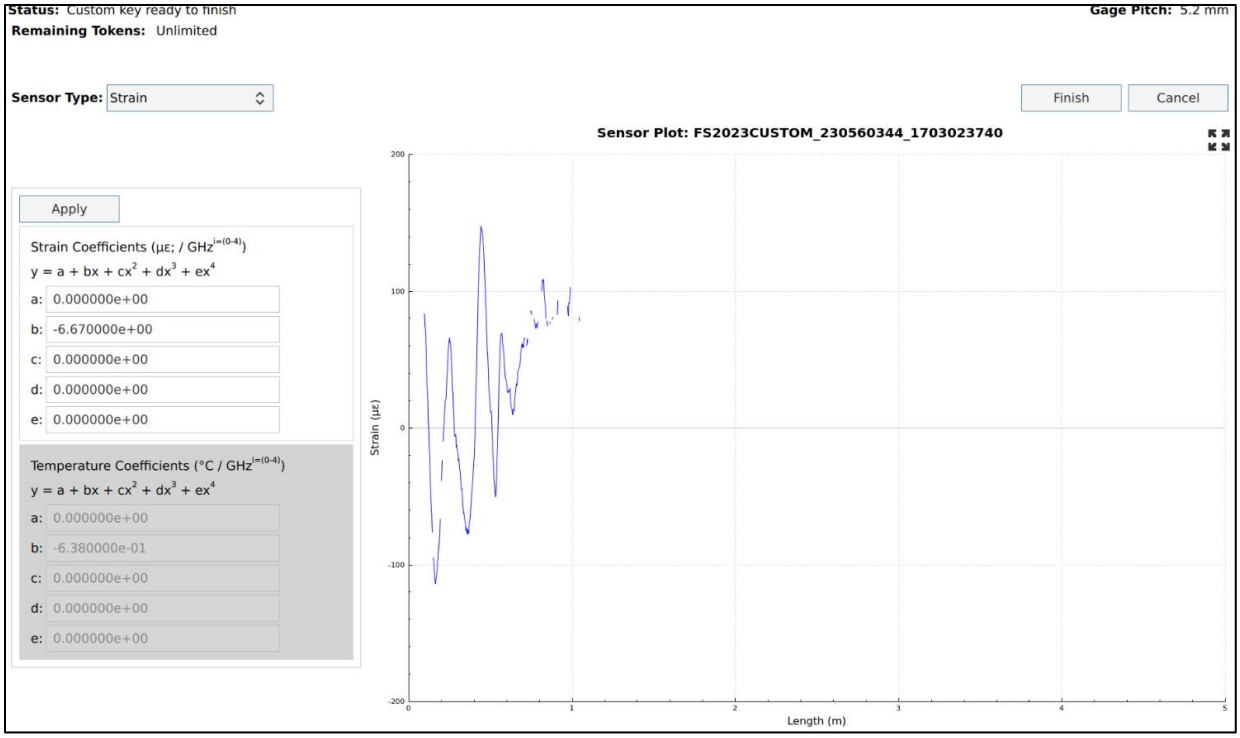

Figure 7. Sensor interrogator calibration coefficients.

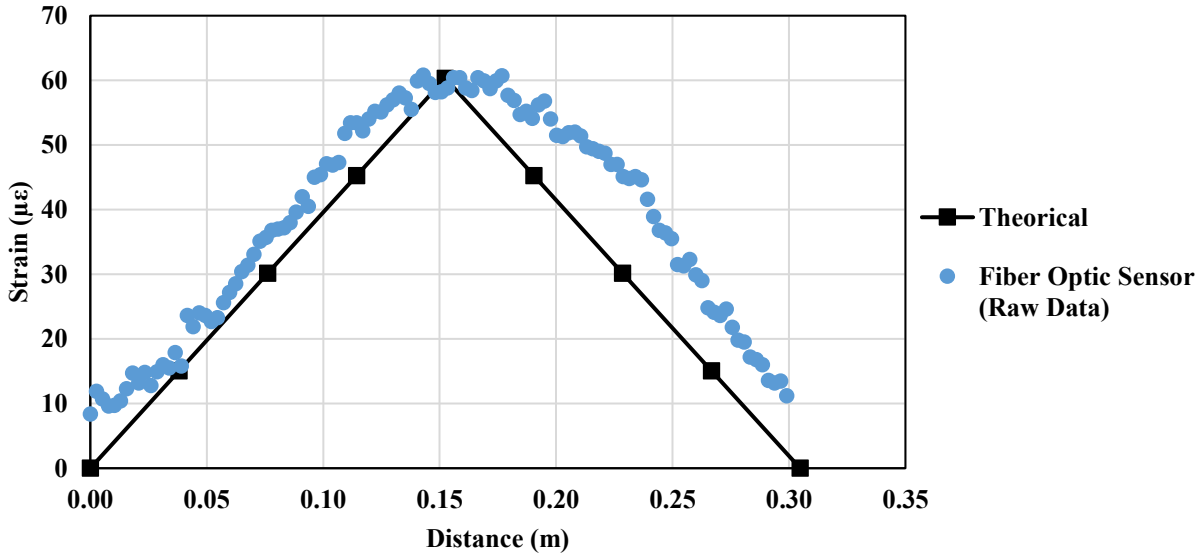

Figure 8. Sample raw strain measurements of three-point bending test of aluminum jig specimen.

Chapter 5. Accelerated Pavement Testing and Results using DFOS and MMLS

To implement DFOS for laboratory-scale accelerated pavement testing, the research team proceeded to prepare the test setup to conduct a series of tests utilizing a Model Mobile Load Simulator (MMLS). The MMLS is a device designed to simulate pavement behavior under load, suitable for both field use on actual pavement and laboratory testing on a scaled model. The MMLS measures 95 in. (2400 mm) × 24 in. (600 mm) × 45 in. (1150 mm) and weighs 1760 lb (7.8 kN). Its loading system features four bogies, each equipped with a single axle and wheel, as shown in Figure 9. The wheels feature 3.2 in. (80 mm) wide tires designed to withstand a maximum pressure of 116 psi (800 kPa), capable of handling axle loads ranging from 430 lb (1.9 kN) to 600 lb (2.7 kN). Tests were conducted using a 600 lb load. Operating at a speed of 8.2 ft/s (2.5 m/s), the device delivers a nominal wheel load application rate of 7200 passes per hour (Bhattacharjee et al. 2005).

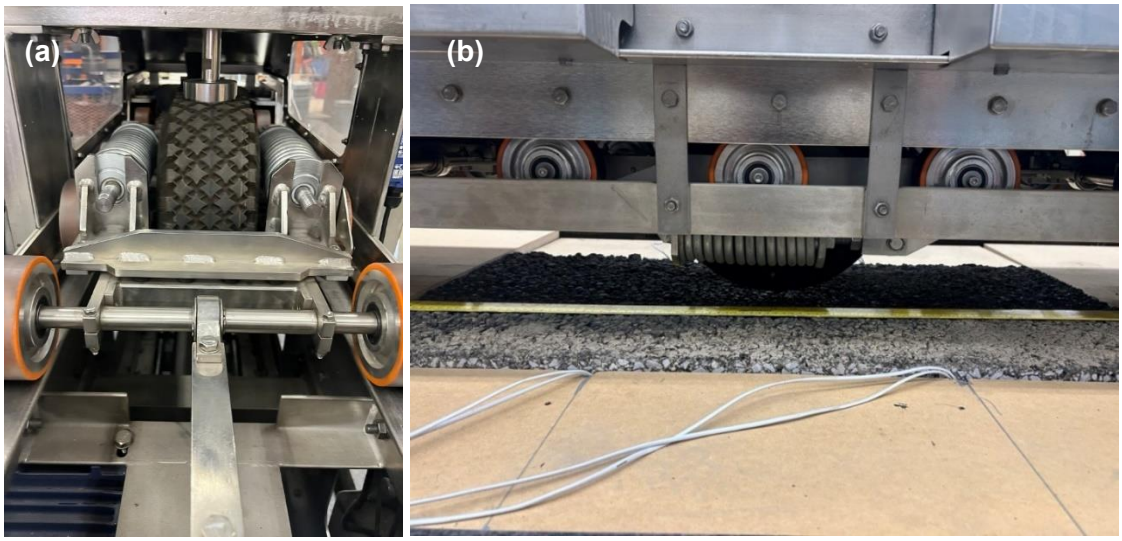

Figure 9. (a) Closeup front and (b) side views of MMLS system showing a single wheel.

Load adjustments were performed by modifying the axle spring system, while tire pressure was controlled through inflation/deflation, to maintain an operating pressure of 100 psi. A scaled load of 600 lb (2.7 kN) was applied to the compacted asphalt slabs.

To simulate a three-layered pavement structure, a 3-in. asphalt slab was laid on top of two additional layers representative of a base course and subgrade. For this purpose, three 1-in. neoprene N80 sheets, with a tensile strength of 1.0 ksi, were placed on top of a 3-in. layer of compacted soil, as shown in Figure 10. Both the soil and asphalt slab were compacted using a hand-driven steel roller.

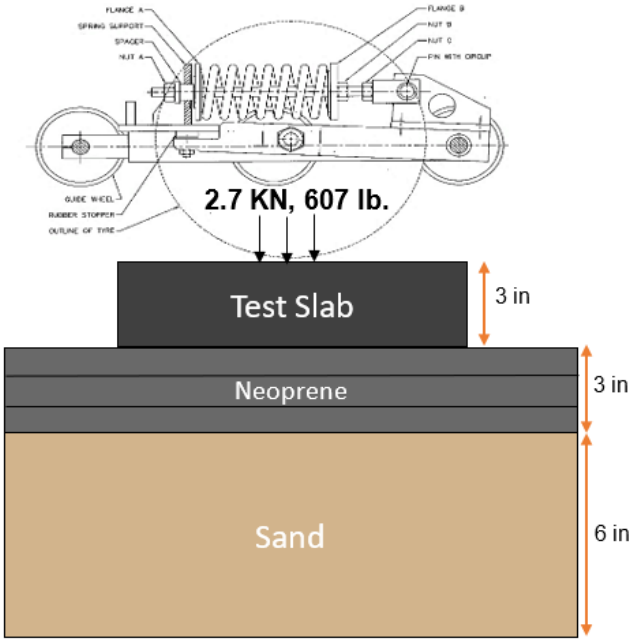

Figure 10. Schematic with dimensions of asphalt specimen on top of supporting structure utilized for MMLS testing.

To refine the test setup and improve the quality of the results, various asphalt specimens were constructed and instrumented with terminated and calibrated fiber optic strain sensors in place. These sensors were installed both longitudinally and transversely within the asphalt slabs. The MMLS system was positioned directly above each specimen. To investigate the capability of the strain sensors in measuring the induced strains to traffic loads, cyclic wheel passes were conducted with the instrumented surface facing both upwards (to capture compressive strain responses) and downwards (to capture tensile strain responses).

During preliminary testing, the research team encountered challenges, including non-uniform strain responses primarily attributed to:

- *Cantilever effects:* The slab exhibited some cantilever behavior due to inadequate support or anchoring to the underlying material.
- *Sensor detachment:* In some cases, the fiber optic sensor exhibited loose sections due to insufficient bonding along the length of the slab specimen, particularly at the ends.

These initial observations led to refinements in the MMLS test setup, including the evaluation and optimization of different methods to bind the fiber optic sensor within the asphalt slab. For instance, the initial experimental configuration is shown in Figure 11, where the responses were affected by the supporting and securing conditions of the asphalt slab. To address this problem, plywood was introduced to prevent horizontal movement of the asphalt slab. The revised setup is depicted in Figure 12. After finalizing the test setup, the sensor interrogator was again to the embedded fiber optic sensor to allow real-time strain measurements as the MMLS applied accelerated cyclic traffic loads.

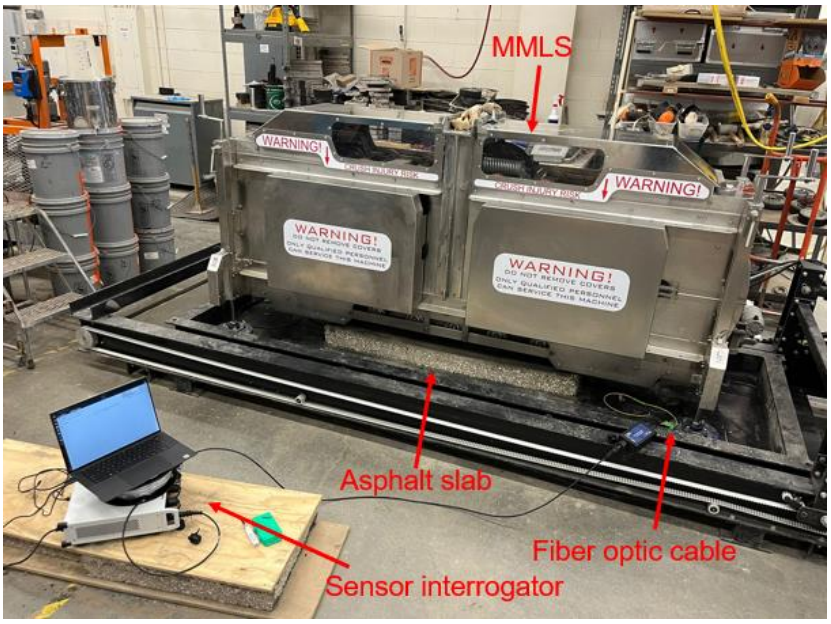

Figure 11. Asphalt slab testing using MMLS (no restraint provided to the asphalt slab).

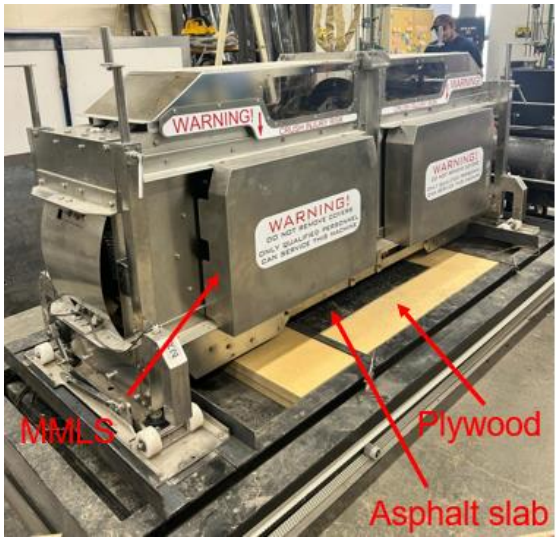

Figure 12. MMLS test setup with restrained asphalt slab.

5.1 Specimen Preparation for Instrumentation for MMLS Testing

To investigate the performance of asphalt under trafficking, a common dense-graded PG 64-22 asphalt was used to compact a 3-in. thick asphalt slab, 3 ft wide and 5 ft long, using the MMLS's drum roller, as shown in Figure 13.

Figure 13. Asphalt slab compaction using MMLS drum roller.

Following compaction, dry ice was applied to the slab surface area around the center of the slab to stiffen the material and minimize the risk of cracking during the cutting process. Using a circular steel saw, the slab was cut to dimensions required for testing and then carefully extracted, as shown in Figure 14. To ensure secure placement and prevent any movement during subsequent handling, installation, and loading, the fiber optic cable was carefully adhered to the groove using epoxy. A view of an asphalt slab specimen instrumented transversally with the fiber optic strain sensor is seen in Figure 15. To obtain tensile strain measurements, the instrumented asphalt slab was turned upside down and placed on top of the neoprene sheets. As mentioned before, plywood boards were installed to prevent lateral movement of the slab specimen and tack coat was applied to bind the neoprene pads to the asphalt slab. The instrumented asphalt slab setup under the MMLS is shown in Figure 12.

The sensor interrogator system was then connected to the instrumented fiber optic cable to obtain strain measurements, as was shown in Figure 11, to be subjected to accelerated trafficking loads as soon as the MMLS is turned on.

Figure 14. Cutting asphalt slab.

Figure 15. Fiber optic cable instrumentation on asphalt slab.

5.2 Test Results and Discussion

Proper compaction, instrumentation, and test setup are crucial to obtain proper fiber optic strain results. The research team acquired measurements using an asphalt slab to obtain raw data and identify means to reduce collected data. The system's acquisition rate of 125 Hz, coupled with a gage pitch of 2.6 mm, results in substantially large data files that required additional processing to reduce data and identify the relevant information. Figure 16 presents raw strain measurements along the length of fiber optic sensor instrumented at the bottom of a conventional dense-graded PG 64-22 asphalt slab, within the pavement structure described in Figure 10. The figure shown depicts a concentration of tensile stress directly beneath the wheel load. The measured strain profile aligned well to a certain extent with the expected pattern along the slab length. However, within the final 0.4 m (16 in.) of the slab, the strain sensor unexpectedly registered compressive strain. This deviation may be attributed to the potential separation between the slab and the supporting neoprene pads at the edge, or to possible inadequate bonding between the fiber optic sensor to the slab surface. This phenomenon was more pronounced in earlier compacted slabs, as both edges exhibited this behavior. Refinements in our methodology, including improvements to the fiber optic sensor bonding process and enhanced securing measures to prevent lateral movement of the slab, resulted in improved quality of data. However, as shown below, compressive strains were still observed towards one end of the slab, always on the departing edge, despite the efforts in improving the experimental and instrumentation setup.

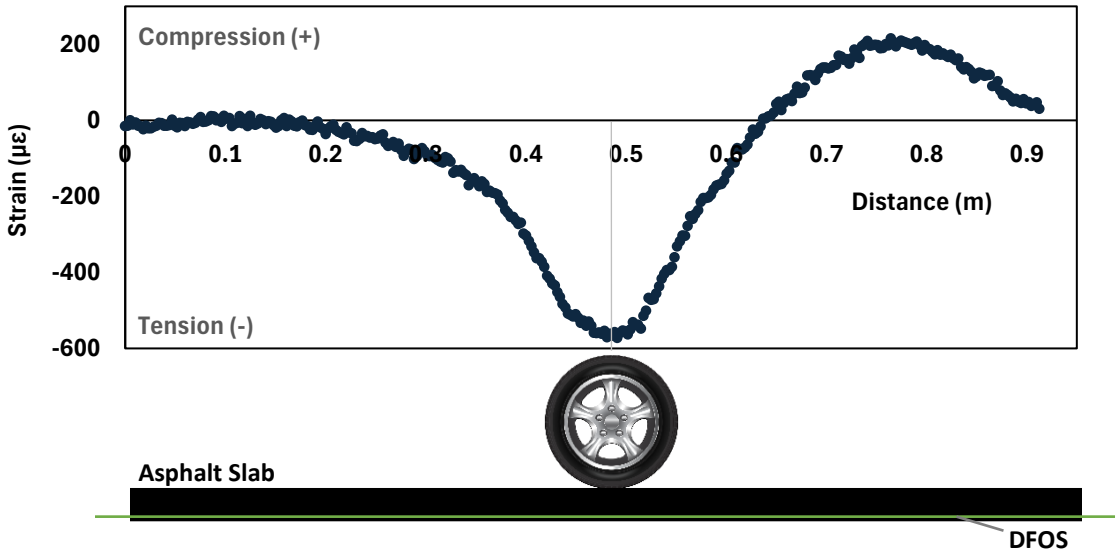

Figure 16. Fiber optic strain response measurements when tire passes through the middle of slab.

Figure 17 and Figure 18 show different strain responses as measured by the fiber optic strain sensor at different intervals, as the tire rolls from one end of the slab towards the other. Both figures demonstrate that peak tensile strains consistently occur directly underneath the wheel load. While peak tensile strain values remain relatively consistent in magnitude along the first half of the slab; a significant increase in magnitude is observed beyond the mid-point (Figure 18b-g). This increase in strain response may be attributed to potential support-related issues, as previously discussed. An envelope of the peak tensile strains for this MMLS pass is shown in Figure 19, generated by identifying peak tensile strains at the specified cycle shown in the previous figures from measurements taken at 2.6 mm along the slab. Three sets of measurements are superimposed at different intervals showing the position of the tire along the slab for reference.

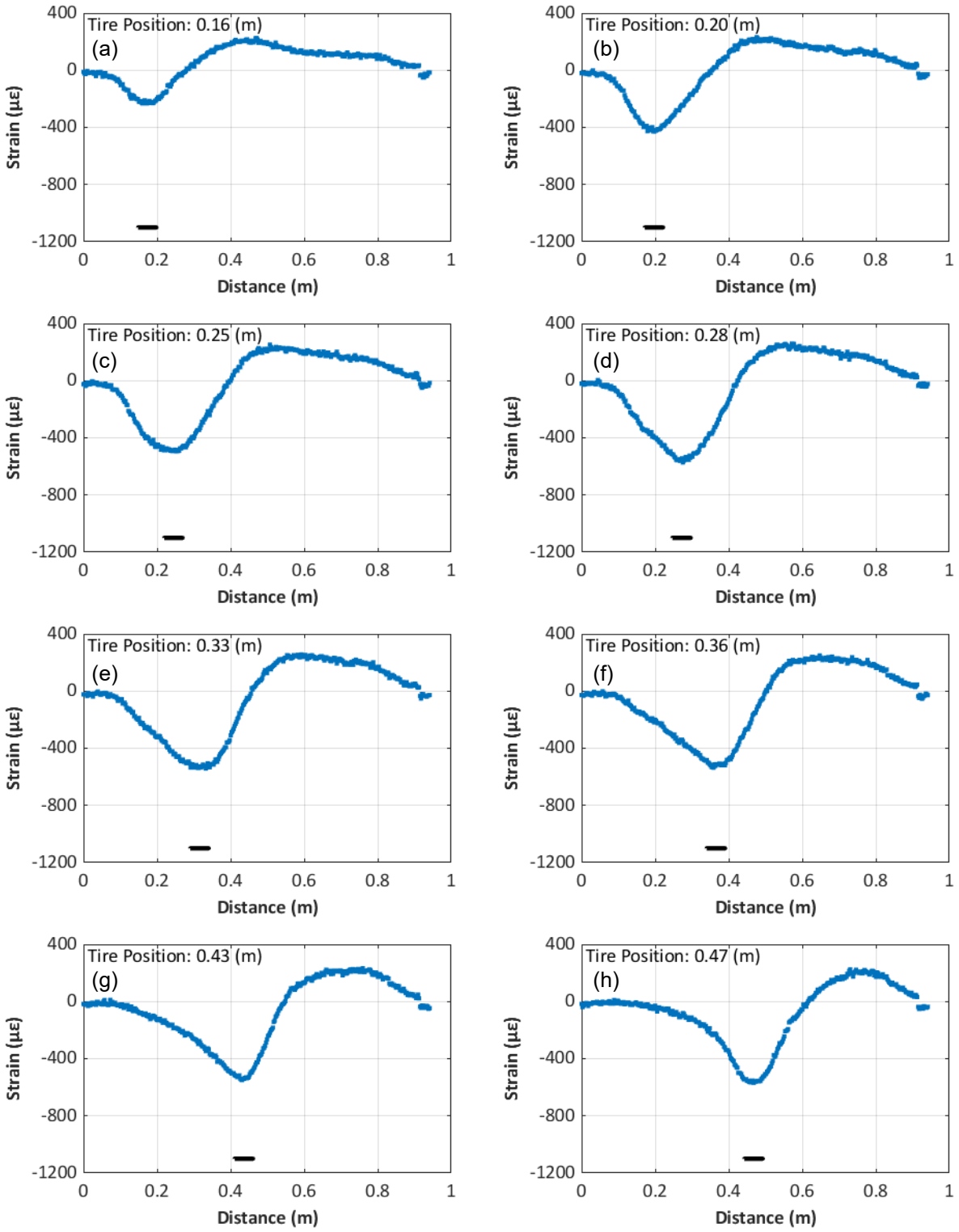

Figure 17. Fiber optic strain response measurements with peak tensile strain (negative) values directly under tire, at different positions (a-h) approaching from edge towards middle of slab.

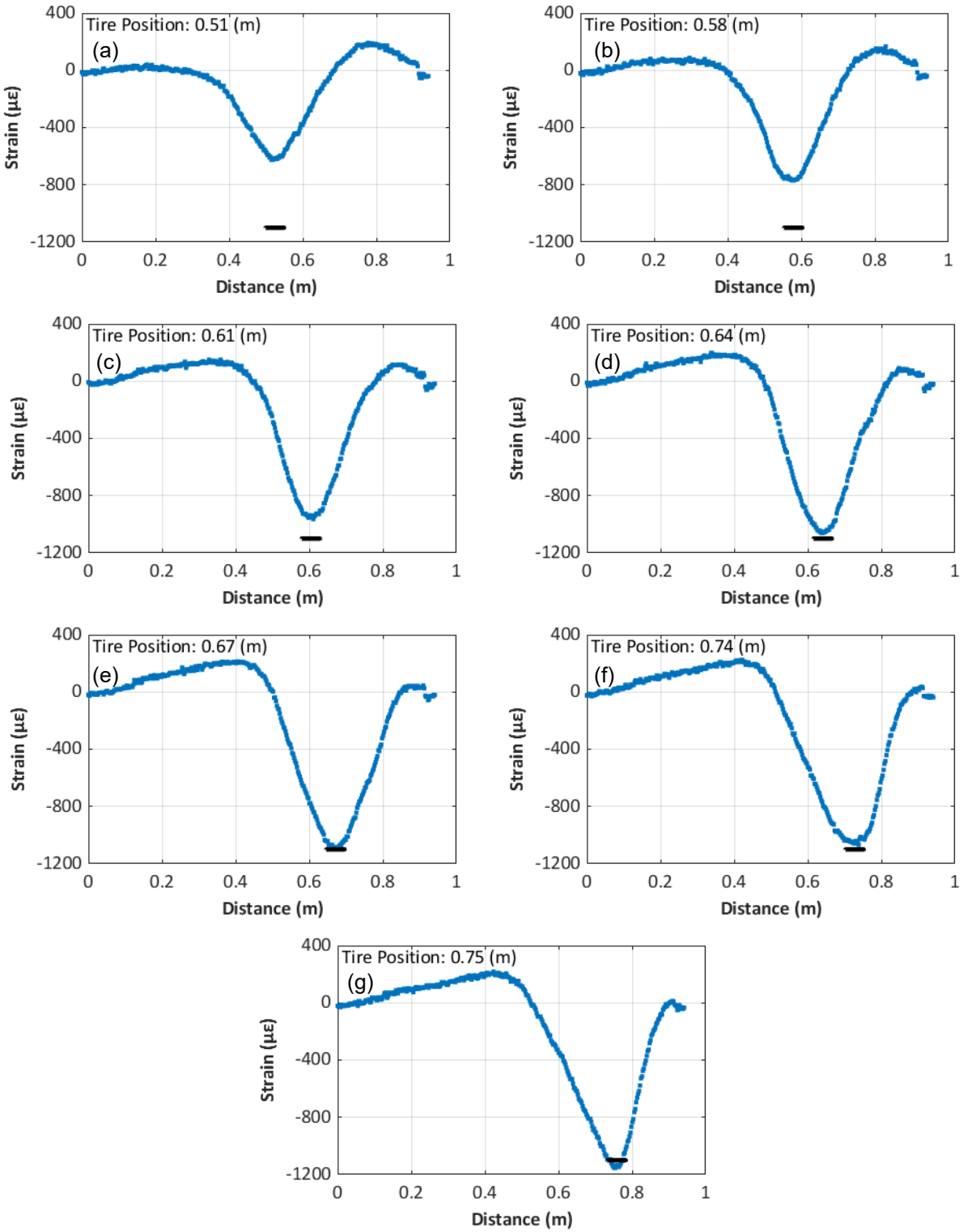

Figure 18. Fiber optic strain response measurements with peak tensile strain (negative) values directly under tire, at different positions (a-h) moving away from middle of slab towards edge of slab.

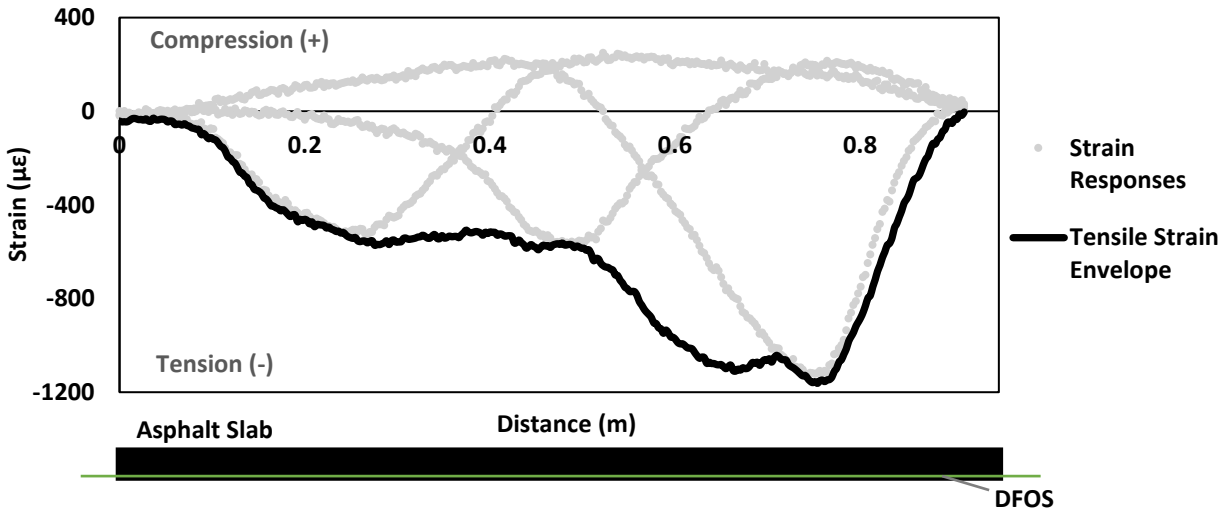

Figure 19. Envelope of Tensile Strains.

As previously discussed, strain sensing measurements offer a significant advantage by readily identifying potential issues with the test setup or instrumentation. Unexpected strain patterns, readily apparent when using fiber optic sensors, provide valuable diagnostic information. In contrast, conventional strain gauges, limited to point measurements, complicate data interpretation as these are unable to show the response simultaneously at different locations, unless multiple ones are installed. For instance,

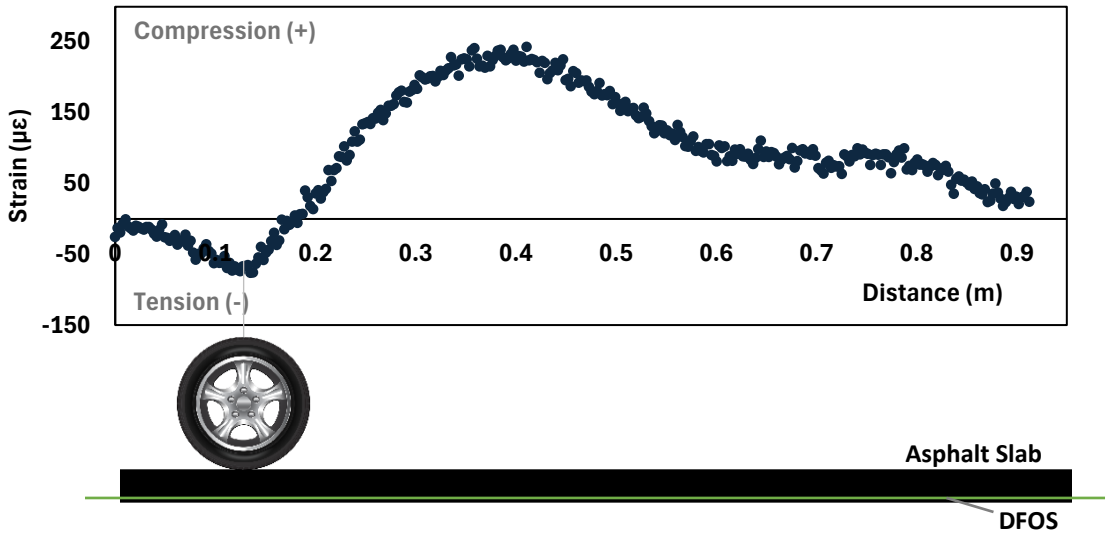

Figure 20 shows the strain response when inadequate bonding of the fiber optic sensor and poor securing leading to slab detachment at one end induced a cantilever-like behavior as the load is applied at the opposite end. While pinpointing the exact cause of such anomalous behavior can be challenging, potential contributing factors include inadequate sensor bonding to the asphalt slab, improper compaction of the slab, and/or insufficient tack coat application between the neoprene layer and the asphalt slab.

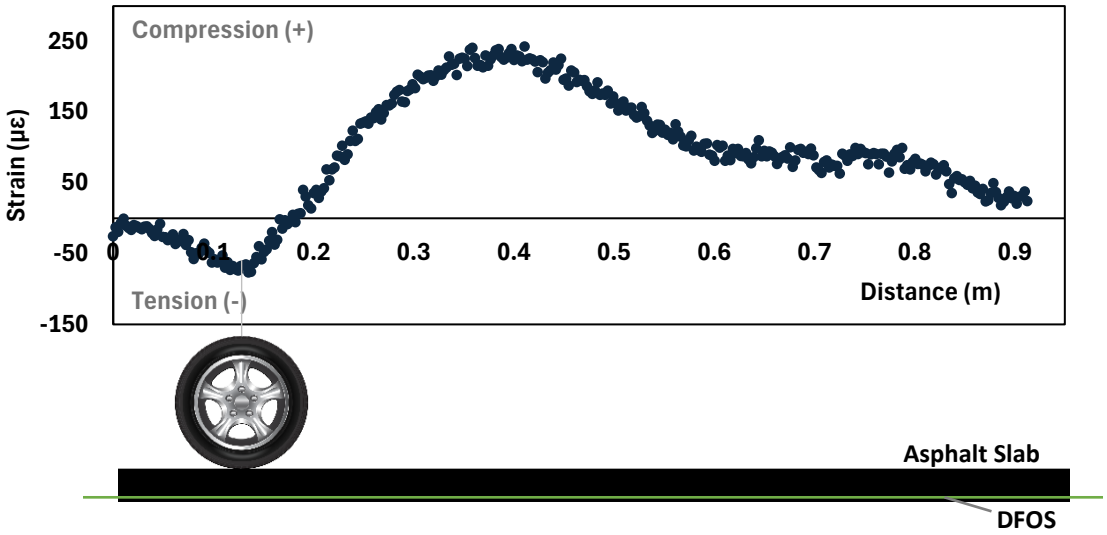

Figure 20. Anomalous fiber optic strain response of a slab with inadequate support and sensor integration.

To effectively analyze the collected data and assess the response measurements, data improvement techniques were employed to minimize noise. While moving averages were considered, Gaussian smoothing was ultimately preferred due to its ability to effectively smooth fluctuations while preserving the overall shape of the data. This approach enhanced data clarity and facilitated interpretability without compromising measurement accuracy, as shown in Figure 21. However, as the research team refined the sensor integration process, the necessity for extensive data smoothing diminished.

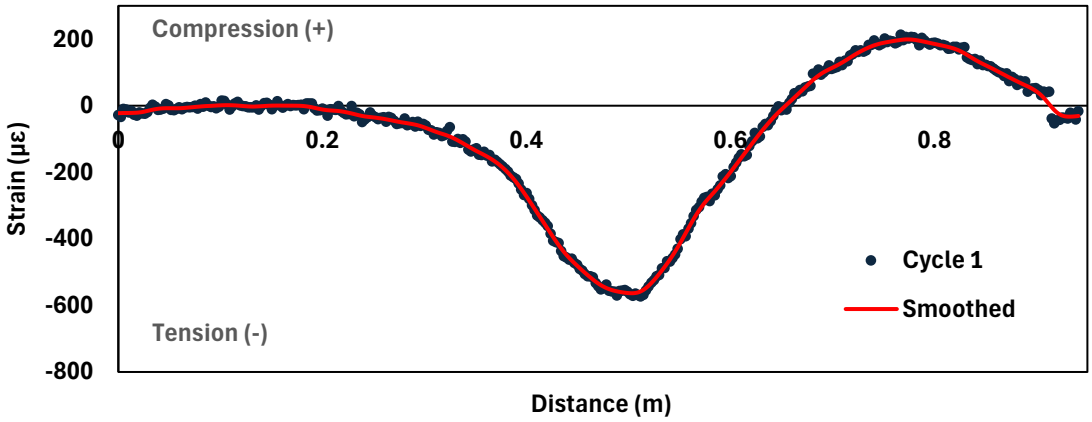

Figure 21. Smoothing of measurements to reduce noise.

Figure 22 shows multiple responses at different tire positions and cycles from one of the earlier tests. These measurements revealed the need for significant improvements to the experimental

setup before proceeding with an assessment of measurement variability. These improvements included incorporating epoxy to bind the strain sensor to the slab, securing the asphalt slab to the underlying neoprene sheet with epoxy, improving the compaction process to achieve a more uniform slab despite limitations under laboratory conditions, minimizing lateral and vertical slab movement through improved restraints, and limiting MMLS movement. These measures were implemented to ensure more consistent measurements.

Figure 23 shows strain measurements from three consecutive passes at the same tire position, acquired after implementing significant improvements to the test setup and instrumentation. Despite these improvements, a variability of about 12% is observed in peak strain values on these three cycles. Further investigation is required to differentiate between measurement variability inherent to the test setup and variability arising from material behavior (e.g., ongoing compaction).

These refinements to the experimental and instrumentation test setup required significant iterative adjustments. This limited the scope of further experiments and the ability to comprehensively assess measurement variability. To further validate the reliability of the fiber optic sensor's strain measurements, the research team was still in the process of integrating conventional strain gauges into the calibration jig and directly onto the asphalt surface at the time of report completion.

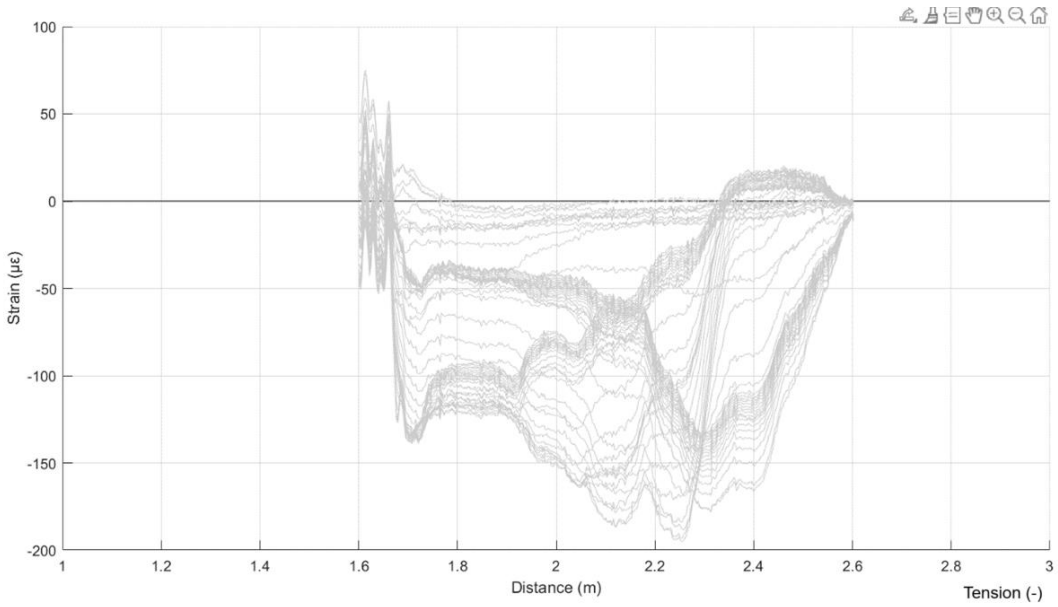

Figure 22. Strain results on asphalt slab during MMLS trafficking test.

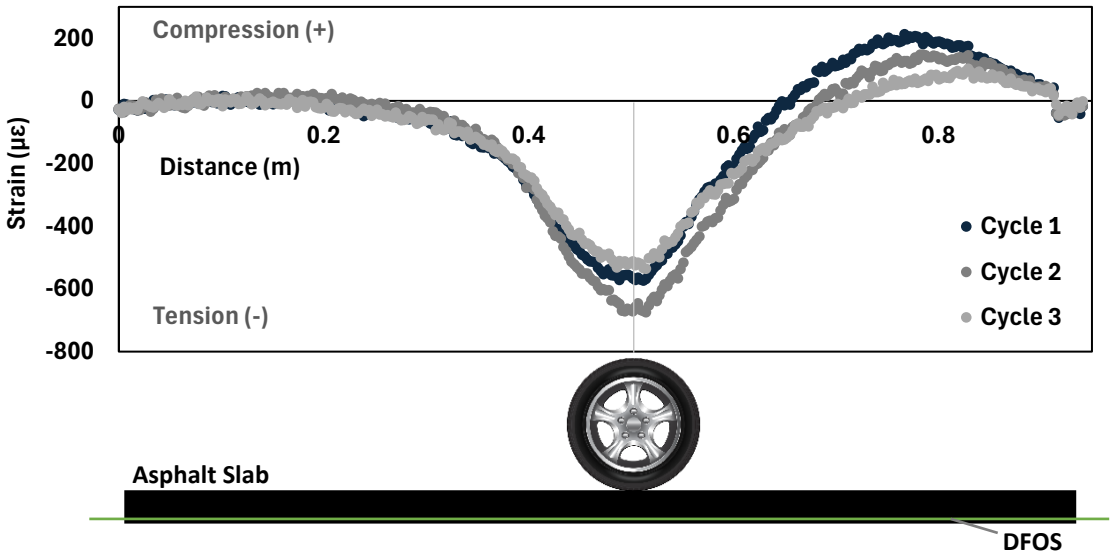

Figure 23. Strain results showing multiple cycles with tire located at the middle of slab.

Despite the influence of factors such as slab securing, strain sensor bonding to the slab, among other setup conditions, on the repeatability of measurements, some loading positions yielded repeatable measurements at the same location. For instance, Figure 24 shows the time history of a specific location along the strain sensor during one test case, which exhibited consistent, repeatable measurements. This suggests that the strain sensor itself can provide reliable and repeatable measurements, provided that controlled conditions are implemented: consistent compaction procedure, test setup to prevent movement and achieve stable tests, and proper instrumentation setup to ensure the fiber optic sensor remains securely in place and in contact with the pavement material.

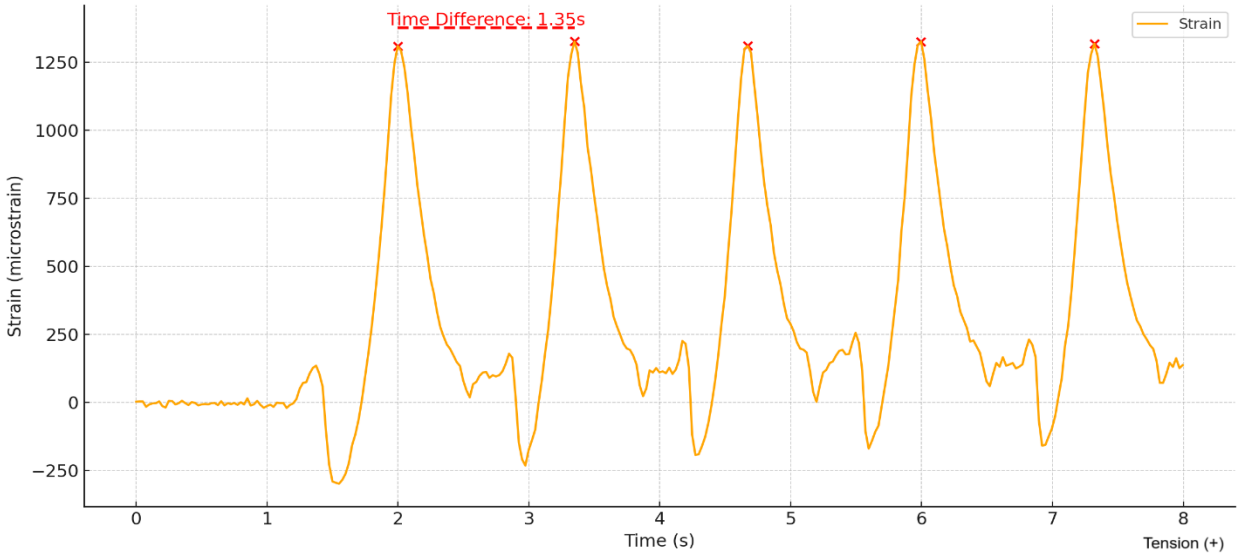

Figure 24. Strain response time history at one point.

Chapter 6. Conclusions and Recommendations

This research aimed to develop and implement protocols for instrumenting pavements using distributed fiber optic strain sensing by conducting tests for measuring strain in asphalt slabs subjected to accelerated laboratory-scale pavement testing. Initial efforts involved developing a dedicated jig to perform a three-point bending test for calibrating the fiber optic strain sensor. The calibrated fiber optic strain sensor was then integrated into asphalt slab specimens tested using a Model Mobile Load Simulator (MMLS) to measure strain responses when subjected to accelerated traffic loading.

It can be concluded that fiber optic strain sensors offer the capability to obtain detailed strain readings at high spatial resolution (at least every 2.6 mm) along the length of the sensor. This demonstrates their potential for measuring strain distributions within pavement structures. Calibration of the strain sensor system using a dedicated jig was successfully achieved. However, challenges related to slab support, sensor bonding, and compaction were encountered and addressed through iterative improvements to the test setup. The distributed strain sensing system proved to be a valuable diagnostic tool, revealing anomalous strain patterns that revealed potential issues within the test setup. Significant variations in strain measurements were observed between different asphalt tests, highlighting the importance of controlled experimental conditions (e.g., testing setup, secure sensor installation) and consistent compaction to minimize variability and ensure reliable and repeatable results.

Despite the use of steel-reinforced strain sensors, a significant drawback of this technology lies in the inherent fragility of its components, particularly those that are non-reinforced exposed sections, such as the spliced connections to patch cables and coreless termination fibers. Damage to the coreless fiber or its connection to the strain sensor can significantly impact the calibration parameters, as re-splicing inevitably alters the length of both the coreless fiber and the strain sensor. While less critical than coreless termination fiber damage, re-splicing patch cables may have an impact on the sensor calibration, though further investigation is required to confirm this and to come up with a procedure to adjust the calibration parameters, considering that the strain sensor can no longer be retrieved after embedment.

To address these concerns and validate the accuracy of distributed strain sensing measurements, additional research is imperative. For instance, integrating conventional strain gauges for independent validation of the fiber optic strain sensor measurements is needed.

Despite the use of reinforced sensors, a drawback of this technology lies in the fact that it is easy to damage, in particular in exposed non-reinforced components, such as the connections between patch cables and strain sensor, and in the fragility of the coreless fiber spliced at the other end of the sensor. It was noted that repair of the coreless fiber seems to affect the calibration parameters, as a different, potentially shorter, length of both the coreless fiber and strain sensor will occur when re-splicing. Though it may not be as critical as the coreless fiber, resplicing of patch cables may also affect the calibration of the sensor; however, further investigation is needed to assert this. Further research is needed to investigate measurement variability, and for this purpose, conventional strain gauges should be integrated for independent validation of the fiber optic strain sensor measurements. Once these items are addressed, the research team recommends investigating the sensitivity of the strain-sensing technology to key pavement distress mechanisms, such as delamination, crack development, and temperature fluctuations impacting modulus in asphalt, among other relevant concerns. An expanded research study will provide valuable insights into the potential of this technology for real-time monitoring and management applications.

Chapter 7. Implementation of Project Outputs

7.1 Introduction

This section outlines draft guidelines for the calibration and installation of distributed fiber optic strain sensors for accurate and reliable pavement strain monitoring. From the outcome of this study, the research team recommends following these guidelines for obtaining high-quality data and ensuring the successful implementation of this technology in pavement monitoring applications.

7.2 Guidelines for Calibrating and Installing Distributed Fiber Optic Strain Sensors for Real-time Pavement Strain Monitoring

7.2.1 Scope

The following methodology outlines the calibration and installation procedures for fiber optic strain sensors embedded within pavement materials. These sensors provide continuous strain measurements along their entire length, capturing the pavement materials' response to applied loads. The user can make use of the smallest spatial resolution of the strain measurements depending on the specific sensor and data acquisition system used in this study (for the equipment utilized in this project, it was as small as 2.6 mm). However, the measurement interval can be adjusted to coarser resolutions to accommodate project requirements and data storage limitations.

7.2.2 Terminology

- **Patch cord:** A flexible optical fiber cable that connects optical devices, such as sensors or communication equipment, to fiber optic network. Patch cords facilitate connections while minimizing signal loss and maintaining performance integrity during strain measurement applications.
- **Strip (stripping):** The process of removing the protective coating (cladding) from a fiber optic cable to expose the glass fiber core. This is a critical step in preparing the fiber for splicing or termination, as it allows for the proper alignment and connection necessary for accurate strain measurements and signal transmission.
- **Cleave (cleaving):** The act of cutting the end of a fiber optic cable at a precise angle to create a smooth, flat surface. This process is essential for ensuring optimal light transmission between fibers during splicing. A clean cleave minimizes losses and reflections crucial for maintaining signal integrity in strain-sensing applications.
- **Splice (splicing):** Refers to the joining of two optical fibers to create a continuous pathway for light transmission. This can be done through various methods, such as fusion splicing or mechanical splicing. In the context of strain measurement, splicing is critical for integrating sensors into fiber optic systems, allowing for accurate and reliable data collection.
- **Core Alignment Splicer:** A specialized device used in fiber optic technology to join two optical fibers with precise alignment of their cores. This splicing method ensures that the light traveling through the fibers is optimally coupled, minimizing signal loss and reflection. In applications involving strain measurement, core alignment splicing is needed to obtain

a reliable connection that maintains the integrity of the optical signal, allowing for accurate and consistent readings of changes in strain. The process typically involves the use of sophisticated equipment to accurately align the fiber cores before permanently joining them, either through fusion or another splicing technique.

- **Coreless Termination Fiber:** A type of optical fiber that lacks a central core. It is designed specifically for applications such as strain sensing measurement for structural health monitoring.
- **Spectral Shift:** The change in the wavelength of light as it travels through a fiber optic cable due to variations in strain or temperature, depending on the type of sensor.
- **Sensor Interrogator:** An electronic device that sends and receives signals from fiber optic sensors. It interprets and analyzes the light signals transmitted through the fiber, enabling the measurement of parameters such as strain or temperature, depending of the type of sensor.
- **Attenuation:** Gradual loss of signal strength as light travels through the fiber optic cable. This phenomenon can occur due to bending, micro-bending, and absorption. It may impact the accuracy and sensitivity of strain measurements, as it weakens the signal and may potentially introduce noise.

7.2.3 Procedure

Before installation, the fiber optic strain sensor must undergo calibration. For this purpose, preliminary arrangements are crucial for successfully obtaining reliable measurements after calibration. These preparations include determining the precise length of the fiber optic sensor required to cover the desired monitoring section within the pavement structure. Furthermore, fiber optic splicing is necessary: at one end, a coreless fiber segment is typically spliced to the sensing fiber. This coreless section acts as a reference point for the optical time-domain reflectometry (OTDR) measurements performed by the distributed sensor interrogator. At the other end, the fiber is connected to a compatible connector, ensuring seamless integration with the specific model of the optical distributed sensor interrogator employed for data acquisition. These preparatory steps are essential to establish a stable and reliable baseline for accurate strain measurements during subsequent calibration and field deployment.

7.2.4 Sensor Preparation for Calibration

The following preliminary arrangements are needed:

- **Define Project Requirements and Length Determination:** Specify the desired accuracy, sensitivity, and measurement frequency for the strain monitoring application. The precise length of the sensing fiber is determined based on the specific monitoring section within the pavement structure.
- **Obtain Detailed Sensor Specifications:** Request and review the manufacturer's specifications for the selected distributed fiber optical strain sensor system, including calibration procedures, installation recommendations, and environmental limitations. If available in the manufacturer’s specification, identify strain levels without damage or significant performance degradation and whether the temperature range of operation of the fiber optic sensor is within the temperature range of the application. If sharp bends are expected, identify in the manufacturer’s specifications the minimum bend radius that can be used without significant signal degradation.

- **Coreless Fiber Splicing:** A 200 to 250 mm coreless fiber segment should be spliced to one end of the sensing fiber. This coreless section serves as a reference point for the OTDR measurements conducted by the distributed sensor interrogator. The OTDR technique measures the time it takes for light pulses to travel along the fiber and back, enabling precise location of strain events along the fiber's length. The presence of the coreless fiber provides a distinct boundary for the OTDR measurements, facilitating accurate strain localization. To ensure a precise splice, the coreless fiber should have a core diameter that matches that of the fiber optic strain sensor. The splicing of two fiber optic cables or a coreless termination fiber consists of a process consisting of stripping, cleaving, and splicing the cables. This is done using a fusion splicer with core alignment features.
    - Note: In this research study, the core size of the coreless fiber was carefully selected to match the core size of the strain fiber optic sensor, i.e. 125 µm.
  - Strip manually by carefully removing about 800 mm (i.e., 400 mm to cover the length of the clamp plus 400 mm of exposed cladding) the protective coatings of the fiber optic sensor consisting of the outer jacket and buffer layers from one end of the fiber optic cable using a stripping tool, as the one shown in Figure 25 one diameter of the tool at a time. If the fiber optic cable is reinforced, then the reinforcement must be cut by hand using a knife or a similar tool for the fiber optic cable to be exposed. Proceed carefully until the core is exposed.
    - Note: If a fusion splicer or an alternative device with a strip feature is available, just manually strip to the cladding or outer layer and allow for the fusion splicer to strip the cladding to expose the core.

Figure 25. Stripping tool.

  - Repeat the procedure for the coreless fiber to expose the bare glass. The length of the coreless termination should be about 250 mm (not less than 150 mm and not more than 300 mm).
    - Note: This research used a core size of 125 µm to match the core size of the strain fiber optic cable.
  - Repeat the stripping process for both the fiber optic sensor and the coreless fiber using the fusion splicer (if the unit has such feature, this is preferred). The stripping feature of the fusion splicer will remove the cladding to expose the core of both fibers.
  - Cleave the end of both fibers at the correct angle using a cleaver.
  - Carefully clean the exposed fiber ends with isopropyl alcohol and lint-free wipes to remove any dust particles that could interfere with the splice.
    - Note: Maintaining a clean working space and using clean tools and materials is essential to prevent contamination.

- Using the high-quality core alignment fusion splicer, align the two prepared fiber ends, and clamp the aligned fibers in the splicing device.
- Use the fusion splicer to splice the coreless fiber to the fiber optic sensor. Place both fibers on the splicing plates and cover them with their protective covers to perform the splicing.
    - Note 1: The success of the splice relies on the skill and experience of the individual performing the procedure. Several attempts may be needed to practice and improve this skill.
    - Note 2: Mechanical splicing may be used using precision-engineered sleeves; however, the literature indicates that this procedure may have higher insertion loss. This study did not use mechanical splicing procedures.

- **Connector Termination:** The opposite end of the sensing fiber is connected to a compatible connector. The connector consists of a push-pull connector with a clip-lock mechanism that secures the connector in place to the sensor interrogator. This connector ensures seamless and reliable connection to the specific model of the optical distributed sensor interrogator used for data acquisition and analysis. The choice of connector depends on the interrogator model and the desired level of protection for the connection. To prepare the connection, a patch cord with the same fiber core size (e.g., diameter) of the fiber optic strain sensor core size for a precise splice is needed. To ensure a high-quality connection with low insertion loss, the following steps are needed:
    - Prepare the patch cord first. For this purpose, cut one end of a conventional single-mode pigtail fiber optic cable that comes with a pluggable connector suited for the distributed sensor interrogator. The length of the patch cord will depend on the specific installation requirements and the distance between the sensor and the interrogation system. Typically, LC/APC connectors are typical in fiber optic systems. An APC (Angled Physical Contact) connector end is recommended and used by manufacturers for most strain sensing applications due to its low back reflection. If sharp bends are expected, identify in the manufacturer's specifications the minimum bend radius that can be used without significant signal degradation.
        - Note: The research team identified LC mechanical connectors as an alternative method for directly connecting the fiber optic sensor to an LC connector, eliminating the need for a patch cord (pigtail). However, this option was not evaluated in the current study
    - Strip, i.e. carefully remove about 800 mm of the outer jacket and buffer layers from both the fiber optic sensor and the patch cord exposing the cladding.
    - Strip the exposed cladding using the core alignment splicer to expose the core fiber.
    - Cleave the end of both fibers at the correct angle using a cleaver.
    - Using the core alignment splicer, align the two prepared fiber ends, and clamp the aligned fibers in the splicing device.
    - Use the fusion splicer to splice the patch cord to the fiber optic sensor.
        - Note: The splice should be inspected for any imperfections or gaps, though it is preferred and recommended to use an OTDR to inspect the splice for any imperfection or gap and provide information about the insertion loss of the splice. The research team was able only to obtain the information about the connection loss through the software included with the acquired optical sensor interrogator.

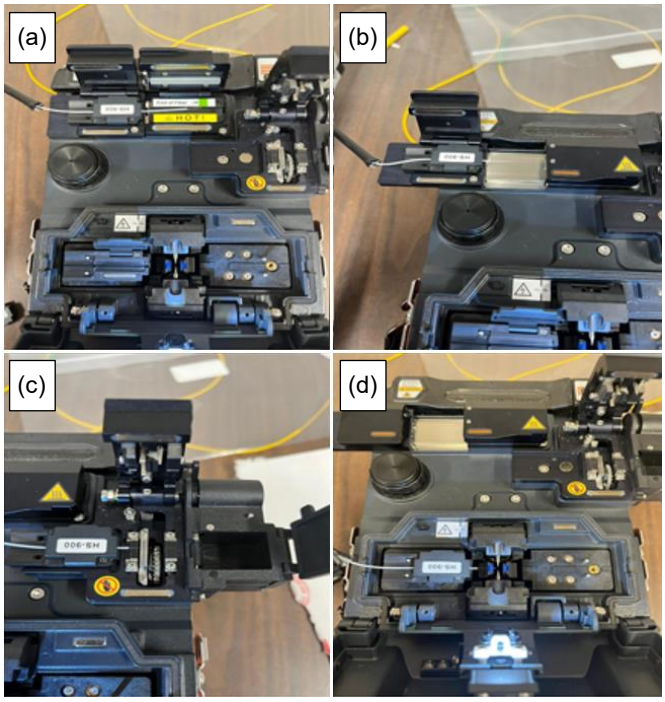

Figure 26. Sequential process of fiber optic splicing consisting of (a) core alignment, (b) stripping protective outer layer, (c) cleaving fiber end, and (d) splicing using fusion splicer.

7.2.5 Calibration of Fiber Optic Strain Sensor

The research team defined these steps to calibrate the fiber optic strain sensor:

- **Test Setup:** Assemble the three-point bending test setup using a 2-in. long aluminum beam jig with a circular groove running longitudinally through the middle of the beam to allow the fiber optic cable to be fully embedded within it. Provide support to both ends of the aluminum to enable a simply supported beam system.
    - Install a segment of the fiber optic sensor within the calibration jig's groove using epoxy adhesive glue to ensure no movement and proper bonding to the jig.
    - Position the jig assembly on an MTS machine. Place the aluminum beam with the fiber optic sensor facing down to obtain tensile strains or facing up to obtain compressive strains, as preferred. The following steps are described for tensile strain measurements.
    - Connect the fiber optic sensor to the distributed fiber optic interrogator following the manufacturer's recommendations.
        - Connect the sensor connector to a remote module (if applicable).
        - Connect the remote module to the standoff cable (if applicable).
        - Connect the standoff cable to the interrogator, following the manufacturer's specifications (if applicable).
    - Connect the computer with data acquisition software to the sensor interrogator.
- **Data Acquisition Setup:** Configure the data acquisition software to collect data in the form of a spectral shift from the interrogator. After this is done the fiber optic cable is connected to the sensor interrogator and a key is created for the new fiber optic cable.

- **Key Creation:** Create a unique "key" for each newly connected fiber. This key allows the interrogator to identify and track the specific fiber within the system.
- **Connection Verification:** The creation of the key will ensure that the light is going through and coming back as supposed to. Upon connection, the interrogator software generates an Optical Frequency Domain Reflectometry (OFDR) plot (Figure 27). This plot provides information about the light propagation along the fiber, including insertion loss, return loss, and potential reflections. In Figure 27, the light is shown as a blue plot and the insertion and return connection and lost values are displayed. If these values are out of bounds, the software will display an error message. Any significant deviations from expected values indicate potential issues with the connection and require re-splicing. If resplicing is necessary, the user will need to create a new key to ensure any changes in the fiber optic cable's length and connection verification values are known by the data acquisition system.

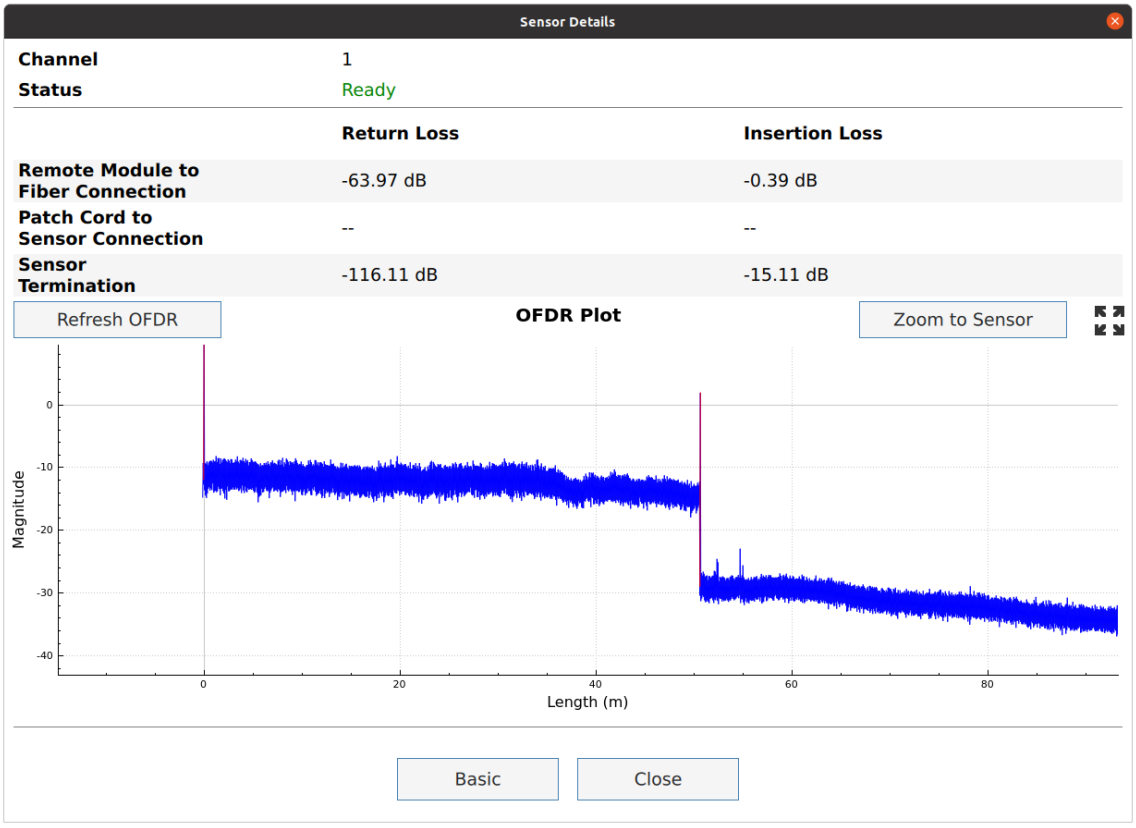

Figure 27. Sensor interrogator ODFR plot.

- **Testing using MTS Loading:** Proceed with the testing. Apply a monotonic load to the beam using the MTS machine.
    - Monotonically increase the load from zero to 5000 lbs.
    - Simultaneously record the applied load and the corresponding spectral shift data from the interrogator.
- **Data Acquisition:** Define the data acquisition requirements:
    - **Data Acquisition Rate** must be set depending on the fiber optic sensor length. Shorter sensors (<2 m) are allowed to acquire measurements at higher rates up to

250 Hz, while longer sensors are set to acquire lower rates up to 100 Hz. The data acquisition software will limit and set the maximum acquisition rate.

- **Gage Pitch:** The gage pitch, or spatial resolution of the strain measurements, is adjustable and could be set by the user to 2.6 mm, 5.2 mm, 7.6 mm, or 1 cm. The selection of the gauge pitch must be set based on the specific requirements of the project.

- **Data Processing:**
  - **Data Extraction (if needed):** A custom code is recommended (can be developed in Matlab, Python, or other preferable programming language) to read the data files generated by the data acquisition system (typically in Excel format) and to reduce the measurements to the ranges of interest, as the files provided by the data acquisition software may be large in size due to the time of testing and the inherent high acquisition frequency used by the device.
- **Calibration:** Export collected spectral shift and applied load measurements in CSV or xlsx format and import into a spreadsheet.

  Determine the theoretical tensile strain measurements at the bottom (or compressive strains at the top) of the aluminum beam, use the sequence of Equations 1 through 5, and fill Table 4, at each applied load. To calculate the theoretical strain ε due to loading P, first determine the bending moment, M, given load P, and the distance X between supports, using Equation 1.

$$M = \frac{P}{4} \times X$$

Equation 1. Maximum Moment of Simply Supported Beam.

Calculate the moment of inertia I and arm y using the aluminum bar's width b and height h, *using*

$$I = \frac{bh^3}{12}$$

Equation 2. Moment of Inertial About the *x*-Axis.

$$y = \frac{h}{2}$$

Equation 3. Moment Arm.

Table 4 – Sample Table for Load to Strain Calculations

Load (lb)	Bending Moment (lb-in.)	Maximum Stress (psi)	Theoretical Strain (με)
0	0	0.00	0.00
500	1500	562.50	56.25
1000	3000	1125.00	112.50
1500	4500	1687.50	168.75
2000	6000	2250.00	225.00
3000	9000	3375.00	337.50
4000	12000	4500.00	450.00
5000	15000	5625.00	562.50

Calculate the corresponding stress σ and strain ε for each load P and bending moment M using

$$\sigma = \frac{M \times y}{I}$$

Equation 4. Stress Calculation.

$$\varepsilon = \sigma / E$$

Equation 5. Strain Calculation.

where E is the modulus of elasticity of the aluminum bar (10,000 ksi or 68.95 GPa for aluminum T-6061).

- Plot a second graph with spectral shift on the y-axis and the calculated strain on the x-axis.
- Fit a linear regression line to the plot of the spectral shift vs strain, and determine the slope ("*b*") and the y-intercept ("*a*") coefficient of the linear equation:

$$\varepsilon = \frac{\text{Spectral Shift} - a}{b}$$

Equation 6. Strain Relationship with Spectral Shift.

as shown in Figure 6.

- **Validate Test:** Conduct a loading test on a material with an embedded fiber optic strain sensor.
  - Use the MTS machine to apply loads and record the corresponding spectral shift data from the interrogator.
  - Convert the spectral shift data to strain values using the calibration equation obtained.
- Compare the calculated strain values to the known or expected theoretical strain values for the test material.
- **Calibration Refinement:** If the calculated strain values do not closely match the known strain values, repeat previous steps to refine the calibration curve. Adjust the loading parameters or data processing techniques as needed to improve the accuracy of the calibration.
- **Removal of Fiber Optic Sensor:** Remove the fiber optic sensor from the calibration jig. Proceed with the next steps to install the calibrated sensor on the pavement materials.

7.2.6 Installing Fiber Optic Strain Sensors in Pavement Materials

As discussed in the previous chapter, this research primarily focused on laboratory-based testing of an asphalt slab subjected to simulated traffic loads utilizing a Mobile Load Simulator (MLS). While the research team initially planned to conduct in-situ testing at the FHWA Turner-Fairbanks Highway Research Center (TFHRC) Pavement Test Facility (PTF), where fiber optic sensors were installed in various pavement test sections, unforeseen challenges arose. Despite the successful installation of the fiber optic sensors and our research team's involvement in verifying their functionality, subsequent changes in management and research priorities within TFHRC, coupled with other unforeseen complications, precluded the continuation of the planned testing at that site within the project timeframe. Nevertheless, valuable insights were gained from a student within our research center who actively participated in the installation of fiber optic sensors at the

TFHRC. These insights have been included in the procedures described in this section regarding the installation of strain sensors into pavement materials.

- **Groove Preparation:**
  - **Laboratory Testing:** For laboratory testing of asphalt or concrete slabs, a groove must be created to accommodate the fiber optic sensor. This can be achieved during compaction by placing a metal cylinder (with the same diameter as the fiber optic cable) on the compaction plate. Alternatively, a circular steel saw can be used to cut a groove with a depth equal to the cable diameter.
  - **Field Testing:** For field installations, prior to placing the surface layer (asphalt or concrete), secure the fiber optic sensor to the underlying base course layer using a tack coat or, preferably, a high-strength adhesive designed for bonding to the base course material (e.g., epoxy adhesives formulated for concrete or bituminous materials). Consult with adhesive manufacturers for specific product recommendations and application guidelines.
    - Note 1: To avoid damage to the fiber optic strain sensor during compaction, the use of a steel-reinforced fiber optic strain sensor is recommended.
    - Note 2: Anchoring or other embedding methods have not been investigated.
- **Cable Embedment:** After carefully placing the fiber optic sensor within the groove, secure it using epoxy adhesive to ensure a strong bond between the fiber optic sensor and the asphalt. Figure 28 depicts the fiber optic sensor embedded in the asphalt.

Figure 28. Embedment of strain fiber optic cable into asphalt.

- **Fiber Optic Cable Preparation:**
  - If the fiber optic sensor is damaged during installation or transportation, it will be necessary to identify the location of the damage and perform splicing of the broken ends. For this purpose, it will be necessary to strip the fiber optic sensor at the damaged location and repeat the procedure of cleaving and splicing the ends of the sensor.
- **Proceed with Testing:** Proceed with the data acquisition and processing to acquire strain sensor measurements, as outlined above in the calibration section. Data reduction may be needed to select and extract strain measurements from specific time intervals and locations of interest, such as the area where the fiber optic sensor was embedded within the pavement material. Measurements are provided along the whole extent of the fiber

optic sensor. To identify a location, a tare can be generated in the software (by touching the strain sensor) and marked as a tare when a change in the strain is identified due to the pressure applied to the sensor. This will help identify the starting point or ending point of measurements.

- **Data Visualization:** Develop or utilize a code to generate a live graph that plots the strain measurements over time, providing a real-time visualization of the strain distribution along the fiber. Appendix A provides a sample code that can be followed and adapted to read strain measurements and visualize the results.

Chapter 8. Technology Transfer and Community Engagement and Participation (CEP) Activities

- A poster was prepared for an exhibit to showcase the research objective, activities, and results to students participating in the Transportation Research Immersive Program (TRIP) Summer 2024 program, organized by SPTC and the Center for Transportation Infrastructure Systems (CTIS) at UTEP on June 19, 2024.

Chapter 9. Invention Disclosures and Patents, Publications, Presentations, Reports, Project Website, and Social Media Listings

- Sebastian Morales, Soheil Nazarian, Rajib Mallick and Cesar Tirado. “Use of Distributed Fiber Optic Sensing (DFOS) for Structural Health Monitoring of Asphalt Pavements,” presented at Infrastructure Advancement Institute (IAI) Summit, Denton, TX, August 2024.

References

Bhattacharjee, S. (2005). *Use of accelerated loading equipment for fatigue characterization of hot mix asphalt in the laboratory* (Doctoral dissertation, Worcester Polytechnic Institute).
Ekechukwu, G. K., & Sharma, J. (2021). Well-scale demonstration of distributed pressure sensing using fiber-optic DAS and DTS. *Scientific Reports*, 11(1), 12505, doi: 10.1038/s41598-021-91916-7.

Johannessen, K., Drakeley, B., & Farhadiroushan, M. (2012). Distributed acoustic sensing new way of listening to your well/reservoir. In *SPE Intelligent Energy International Conference and Exhibition*, Utrecht, The Netherlands, Society of Petroleum Engineers, pp. SPE-149602, doi:10.2118/149602-MS.

Ghazali, M. F., Mohamad, H., Nasir, M. Y. M., Hamzh, A., Abdullah, M. A., Abd Aziz, N. F., ... & Zan, M. S. D. (2024). State-of-The-Art application and challenges of optical fiber distributed acoustic sensing in civil engineering. *Optical Fiber Technology*, *87*, 103911.

Kou, X. W., Du, Q. G., Huang, L. T., Wang, H. H., & Li, Z. Y. (2024). Highway vehicle detection based on distributed acoustic sensing. *Optics Express*, *32*(16), 27068-27080.

Wang, J., Han, Y., Cao, Z., Xu, X., Zhang, J., & Xiao, F. (2023). Applications of optical fiber sensor in pavement Engineering: A review. *Construction and Building Materials*, *400*, 132713.

Xiang, P., & Wang, H. (2018). Optical fiber-based sensors for distributed strain monitoring of asphalt pavements. *International Journal of Pavement Engineering*, *19*(9), 842-850.

Zhu, H. H., Liu, W., Wang, T., Su, J. W., & Shi, B. (2022). Distributed acoustic sensing for monitoring linear infrastructures: Current status and trends. *Sensors*, *22*(19), 7550.

Appendix A: Code to Visualize Distributed Strain Measurements

Sample code to read optical sensor interrogator file with strain measurements that dynamically plots strain measurements at small intervals of time to generate a movie showing the strain as the moving load moves along the pavement slab.

```
clear all; % Clear all variables from the workspace

% Specify the file name, sheet name, and range of the data
filename = 'ODISI_6000_2024-10-30-22-00-35_ch1_full.xlsx'; % File containing the data
sheet = '1'; % Sheet name in the Excel file
xlRange = 'ALX33:BFK1500'; % Range of data to be read from the sheet

% Read the data from the specified Excel file, sheet, and range
DATA = xlsread(filename, sheet, xlRange);

% Create a matrix with the travel distance
% Distance = DATA(1,:); % (Optional) Assign the first row to the Distance variable

% Delete the distance row to retain only the strain data
DATA = DATA(140:end,:); % Keep rows starting from 140 to the end

% Activate if the previous step is commented out
T = DATA; % Assign the processed data matrix to T

% Smooth the entire matrix results using a Gaussian filter with a window size of 5
T = smoothdata(T, "gaussian", 5);

% Calculate the length of the time vector (number of columns in T)
time = length(T(1,:));

% Define the desired dimensions for the plot in inches
width_inches = 10.75; % Set the width of the plot
height_inches = 4;    % Set the height of the plot

% Create a new figure with the specified size and position
fig = figure("Units", "inches", "Position", [3.0, 4.0, width_inches, height_inches]);

% Set the background color of the figure to white
set(gcf, 'Color', 'w');

% Determine the ranges for the graph in Y (Maximum and Minimum Y)
MaxValue = max(T()); % Find the maximum value of T
MinValue = min(T()); % Find the minimum value of T

% Round the maximum and minimum values to the nearest 100
RoundedMaxValue = ceil(MaxValue / 100) * 100;
RoundedMinValue = floor(MinValue / 100) * 100;

ymax = RoundedMaxValue; % Set the maximum Y-axis limit
ymin = RoundedMinValue; % Set the minimum Y-axis limit

% Determine the ranges for the graph in X (Maximum and Minimum X)
MaxValueInX = max(Distance(1, :)); % Find the maximum value in the Distance array
MinValueInX = min(Distance(1, :)); % Find the minimum value in the Distance array

% Round the maximum and minimum values to the nearest integer
RoundedMaxXValue = ceil(MaxValueInX / 1) * 1;
RoundedMinXValue = floor(MinValueInX / 1) * 1;

xmax = RoundedMaxXValue; % Set the maximum X-axis limit
xmin = RoundedMinXValue; % Set the minimum X-axis limit
```

```
% Set the graph limits and styling
ylim([ymin, ymax]); % Set the Y-axis limits
xlim([xmin, xmax]); % Set the X-axis limits
hold on;            % Hold the current plot to add more elements
grid on;            % Enable the grid for the plot

% Draw a reference line at Y = 0
line([xmin, xmax], [0, 0], 'Color', 'k'); % Add a black horizontal line at Y = 0

% Set the background color of the graph to light gray
light_gray = [0.8, 0.8, 0.8]; % Define light gray color (RGB values)
set(gca, 'Color', light_gray); % Apply the background color

% Loop to update the plot
pause(0.25); % Pause for 0.25 seconds between updates

x = Distance(1, :); % Extract the first row of Distance as x values
Strain = zeros(size(time, length(T))); % Initialize the Strain array with zeros

% Define rectangle center and +/-d
rectCenter = 5.5; % Set the center position of the rectangle
rectDelta = 8;    % Define the width of the rectangle (delta)

% Draw rectangle
rectX = rectCenter + rectDelta * [-1, 1] / 2; % Calculate rectangle's X bounds
rectY = [0.90 * round(ymax), 0.95 * round(ymax)]; % Define rectangle's Y bounds

% Loop through time steps
for i = 1:itime
    % Plot the data
    if imetric == 0 % US units
        xlabel('Distance from edge of PCP (in.)'); % X-axis label
        ylabel('Stress (psi)');                    % Y-axis label
        % Add caption with tire position in inches
        caption = ['Tire position: ', num2str(x(i), '%.2f'), ' in.'];
    else % SI units
        xlabel('Distance (m)');                    % X-axis label
        ylabel('Strain (με)');                     % Y-axis label
        % Add caption with tire position in meters
        caption = ['Tire position: ', num2str(round(x(i), 2), '%.2f'), ' m'];
    end

    if i == 1
        % Plot the data for the first time step
        plot(x(1:i-1), T(1:i-1, :), 'Color', light_gray); % Plot in light gray
    end

    % Plot the data for the current time step
    plot(x, T(i, :), 'k'); % Plot in black
    hold on;               % Hold the plot for further updates

    % Pause to control the speed of animation
    pause(0.25);
end

% Finalize the plot
plot(x, T(:, :), 'k');              % Plot all data in black
pause(0.25);                        % Pause for visualization
plot(x, T, 'Color', light_gray);    % Re-plot with light gray color
```

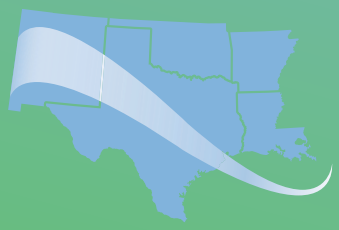

SOUTHERN PLAINS
TRANSPORTATION CENTER

The University of Oklahoma | OU Gallogly College of Engineering
202 W Boyd St, Room 213A, Norman, OK 73019 | (405) 325-4682 | Email: sptc@ou.edu